RESEARCH
ENGINEERING
RESEARCH
ENGINEERING
RESEARCH
ENGINEERING
RESEARCH

ENGINEERING
RESEARCH
INSTITUTE

IOWA STATE
UNIVERSITY
AMES, IOWA

FINAL REPORT

FACTORS INFLUENCING STABILITY OF GRANULAR BASE COURSE MIXES

J. M. Hoover, Project Director

ENGINEERING
RESEARCH
ENGINEERING
RESEARCH

ENGINEERING
RESEARCH

ENGINEERING
RESEARCH

ENGINEERING
RESEARCH

ENGINEERING
RESEARCH

ENGINEERING
RESEARCH

FINAL REPORT

FACTORS INFLUENCING STABILITY
OF GRANULAR BASE COURSE MIXES
J. M. Hoover, Project Director

Iowa Highway Research Board Project HR–99
conducted by
Engineering Research Institute, Iowa State University
for
Iowa State Highway Commission
in cooperation with
Federal Highway Administration,
Bureau of Public Roads

ENGINEERING   RESEARCH   INSTITUTE

Project 516-S
ERI–337

IOWA STATE UNIVERSITY   AMES

CONTENTS

I. INTRODUCTION — OBJECTIVES

To evaluate the various factors influencing the stability of granular base course mixes, three primary goals were included in the project:

(1) determination of a suitable and realistic laboratory method of compaction;

(2) effect of gradation, density and mineralogy of the fines on shearing strength; and

(3) possible improvement of the shear strength with organic and inorganic chemical stabilization additives.

II. MATERIALS

Three crushed stones were used in this project. Each was selected in cooperation with the Iowa State Highway Commission's Director of Research, Materials Engineer and Geologist as being representative of ISHC approved crushed stone for rolled stone bases. The three crushed stones used include:

1. A weathered, moderately hard limestone of the Pennsylvania System, which outcrops about half of the state of Iowa. It was obtained from near Bedford, Taylor County, Iowa, and hereafter is referred to as the Bedford sample. Generally, rock of the Pennsylvanian System is of poor quality, but is the only economically available stone in many regions of the state.

2. A hard concrete quality limestone of the Mississippian System obtained from near Gilmore City, Humboldt County, Iowa. Hereafter it is referred to as the Gilmore sample.

3. A hard dolomite of the Devonian System, of consistent quality, and a valuable source of aggregate in Iowa. Obtained from near Garner, Hancock County, Iowa. Hereafter it is referred to as the Garner sample.

Results of chemical and mineralogical tests of the three stones, as determined by x-ray identification, pH measurement, cation exchange capacity (CEC) and hydrochloric acid-soluble and nonsoluble minerals, are shown in Tables 1, 2 and 3. Table 4 presents the engineering properties of each of the three materials.

In addition to the physical property tests noted in Table 4, porosities (i.e., percentage relation of void volume to total volume) of duplicate ½-in.

diameter by 1 1/2-in. high cylindrical cores and 3/4-in. crusher run parti-
cles were determined by the gas pycnometer method. Quantitatively the
porosity of the Bedford stone was slightly over 32%, while the Garner and
Gilmore stones were about 10 and 12% respectively. The difference in
porosities between the Bedford sample and the Garner and Gilmore samples
is significant.

Table 1. Mineral constituents of the whole material by x-ray diffraction*.

Stone	Calcite	Dolomite	Quartz	Feldspar	Calcite/dolomite ratio[a]
Bedford	Pred.	Small amount	Trace	Not ident.	25
Garner	Pred.	Second pred.	Trace	Not ident.	1.16
Gilmore	Pred.	None	Trace	Not ident.	—

[a] Obtained from x-ray peak intensity.

Table 2. Non-HCl acid soluble clay mineral constituents of the whole
material by x-ray diffraction*.

Stone	Mont.	Vermiculite-chlorite	Micaceous material	Kaolinite	Quartz
Bedford	None	Not ident.	Pred.	Poorly crystalline	Large amount
Garner	None	Small amount	Pred.	Second pred.	Large amount
Gilmore	None	None	None	Pred.	Small amount

*Representative sample was ground to pass No. 100 sieve.

Table 3. Quantitative chemical analysis of whole material[*].

Stone	pH	CEC (me/100 g)	Non-HCl soluble clay minerals (%)	Nonclay mineral non-HCl soluble Material (%)	HCl soluble calcareous material (%)
Bedford	9.40	10.88	10.92	Trace	89.08
Garner	9.25	10.60	5.70	1.03	93.27
Gilmore	8.99	5.86	<1.66	Trace	>98.34

*Representative sample was ground to pass No. 100 sieve.

Table 4. Representative engineering properties of crushed stone materials.

	Bedford	Garner	Gilmore
Textural composition (%)			
Gravel (>2.00 mm)	73.2	61.6	66.8
Sand (2.00 - 0.074 mm)	12.9	26.0	23.3
Silt (0.074 - 0.005 mm)	8.4	10.2	5.9
Clay (<0.005 mm)	5.5	2.2	4.0
Colloids (<0.001 mm)	1.7	1.4	0.9
Atterberg limits, (%)			
Liquid limit	20.0	Non-	Non-
Plastic limit	18.0	plastic	plastic
Plasticity index	2.0		
Standard AASHO-ASTM density:			
Optimum moisture content, % dry soil weight	10.9	7.6	9.4
Dry density, (pcf)	127.4	140.5	130.8
Specific gravity of minus No. 10 sieve fraction	2.73	2.83	2.76
Textural classification	Gravelly sandy loam		
AASHO classification	A-1-b	A-1-a	A-1-a
Unified classification	GW	GW	GW

III. PROBLEM 1 — LABORATORY COMPACTION

The purpose of this study was to ascertain a laboratory compaction procedure which would give uniform, controllable density while minimizing degradation and segregation of the compacted stone samples. The procedures analyzed were:

(1)   standard AASHO-ASTM compaction;

(2)   static compaction;

(3)   vibratory compaction; and

(4)   drop hammer compaction, i.e., molding the whole sample by drop hammering on both top and bottom.

Since the Bedford sample was the least hard of the three materials and has been shown in the field to be representative of the least stability, it was used as the major sample in this study.

A. , Standard AASHO-ASTM Compaction

Triplicate representative samples of the Bedford material were divided into six equal portions, each portion large enough to produce one standard density specimen. The first portion was set aside uncompacted to be used as the control sample for comparison by mechanical analysis. Increasing increments of distilled water were added to each of the remaining portions to produce one point on the M-D curve. Mixing was accomplished by hand to minimize degradation during mixing. Following compaction each specimen was weighed, extruded and examined for visual segregation. Duplicate moisture samples were then removed from each specimen and the remainder was retained for mechanical analysis.

The results of the standard AASHO-ASTM moisture-density study are:

Sample no.	Optimum moisture content (% dry soil weight)	Dry density (pcf)
A	10.4	126.9
B	10.8	128.2
C	11.5	127.1
Average	10.9	127.4

Little visual segregation was noted in the specimens. Density and moisture content variation was within normally accepted limits for each sample.

Table 5 presents a comparison of the average percentage of particle size classifications prior to and following the standard M-D test. The control values are the average of triplicate specimens. The compacted values are the average of all compacted specimens.

Table 5. Comparison of average percentage of particle size fractions before and after AASHO-ASTM standard compaction.

AASHO-ASTM particle Size	Average percentage of particle size (% of total dry sample)	
	Control	Compacted
Gravel	73.2	66.3
Sand	12.9	14.6
Silt	8.4	12.2
Clay	5.5	6.9
Colloids	1.7	1.8

It can be noted that the gravel portion is reduced nearly 7% while the fines content (i.e., minus No. 200 sieve fraction) is increased more than 5% following compaction by this method.

In the three replications of the procedure, for the specimens compacted at less than standard optimum moisture content, the data indicated additional

decreases in percent gravel and a corresponding increase in fines from the average value shown in Table 5. Above standard OMC the samples showed little additional change in degradation from the average noted in Table 5, indicating the lubrication effect of the water.

B. Static Compaction

In this procedure, compaction of the Bedford material was accomplished by application of a load to the top of the sample in a 1/30 cu ft standard AASHO-ASTM mold. The procedure was as follows:

1. Sufficient material, hand mixed to optimum moisture content (10.9%) for maximum standard density (127.4 pcf) in the 1/30 cu ft mold was weighed, placed in the mold, and rodded full depth 25 times with a 0.5 in. diam rod tapered to a dull, rounded point.

2. A 2000 lb load was transmitted to the top of the specimen through a steel piston having an outside diameter slightly under the 4-in. inside diameter of the mold, until the height of the sample was 4.56 in.

3. Triplicate specimens were produced for rates of loading of 0.064, 0.208 and 0.304 in. per minute until the 2000 lb maximum load was reached.

4. Triplicate specimens were also produced for times of maximum load holding of 1, 2 and 5 minutes.

Following compaction, each specimen was weighed, extruded and examined for visual segregation. Duplicate moisture samples were then removed from each specimen and the remainder of the specimen was retained for mechanical analysis.

Segregation of particles was visually obvious in almost all of the statically compacted specimens. No correlation of segregation could be related to the compaction variables due to considerable variation of segregation of the samples within any one compaction condition. In each specimen, water and some fines tended to ooze from around the piston and the bottom of the mold, reducing the moisture content from an initial average of 10.9% to as low as 8.6% (Table 6). Average dry density increased from 0.6 to 1.7 pcf above that obtained by standard AASHO-ASTM compaction. However, the variation of obtained density and moisture content by this procedure was within acceptable limits.

As noted in Table 6, no major effect on degradation was attributable to the variation in loading rates or load holding times. It is obvious, however, that sizeable reduction occurred in the percent gravel, and sizeable increases occurred in all other particle size classes. The following table summarizes the effects of static compaction on degradation.

Compaction condition	Average AASHO-ASTM particle size (% of total dry sample)				
	Gravel	Sand	Silt	Clay	Colloids
None-uncompacted (control)	75.7	9.7	9.6	5.0	1.1
Static load of one ton on 1/30 cu ft sample	62.1	17.9	12.9	7.1	2.5
Average variation of compaction from control	- 13.6	+ 8.2	+ 3.3	+ 2.1	+ 1.4

Table 6. Effect of static compaction variables on particle size degradation.

| Compaction condition	Average dry density (pcf)	Average moisture content (% dry soil weight)	Average AASHO-ASTM particle size (% of total dry sample)				
			Gravel	Sand	Silt	Clay	Colloids
None-uncompacted (control)	-----	---	75.7	9.7	9.6	5.0	1.1
0.064 in./min rate 1 min holding time	129.0	8.9	62.5	17.7	13.3	6.5	2.9
0.064 in./min rate 2 min holding time	129.0	8.9	63.5	17.7	12.2	6.6	2.4
0.064 in./min rate 5 min holding time	129.1	8.6	60.7	18.2	13.8	7.3	2.7
0.208 in./min rate 1 min holding time	128.0	9.6	61.3	18.2	13.4	7.1	2.4
0.208 in./min rate 2 min holding time	128.2	9.5	60.7	19.5	12.3	7.5	2.6
0.208 in./min rate 5 min holding time	128.1	9.8	63.2	16.4	12.8	7.6	2.4
0.304 in./min rate 1 min holding time	128.4	9.6	62.9	18.4	11.2	8.0	2.2
0.304 in./min rate 2 min holding time	128.4	9.7	62.5	16.9	13.6	7.0	2.5
0.304 in./min rate 5 min holding time	128.5	9.4	62.2	17.8	13.2	6.8	2.5

C. Drop Hammer Compaction

To accomplish the objectives of Problems 2 and 3 of the project it was anticipated that 4-in. diam by 8-in. high cylinders would be used. It was considered advisable to ascertain the segregation and degradation effects on 4 x 8 cylindrical Bedford samples compacted similarly to that shown in ASTM Designation D 1632-63, "Making and Curing Soil-Cement Compression and Flexure Test Specimens in the Laboratory." The procedure adopted was as follows:

1. Sufficient material, hand mixed to optimum moisture content (10.9%) for maximum standard density (127.4 pcf) in the 4 in. diam by 8-in. high mold, was weighed, placed in the mold and rodded from the top down until refusal.

2. A separating disc was placed on top of the specimen and compaction was accomplished by dropping a 15-lb hammer (shown in D1632-63) a height of 12 in.

3. The mold was then inverted and the drop hammer was again used.

4. To obtain the proper relationship between standard density and number of blows of the hammer, a series of cylinders were molded using 10, 12, 15, 20 and 30 hammer blows on each end of the specimen.

Following compaction, each specimen was measured for height, weighed, extruded and examined for visual segregation. Slight segregation of the fines was noticeable at each end of the specimens. Duplicate moisture samples were then removed from each specimen and the remainder was retained for mechanical analysis.

Figure 1 shows the relationship between dry density and the number of

FIGURE I
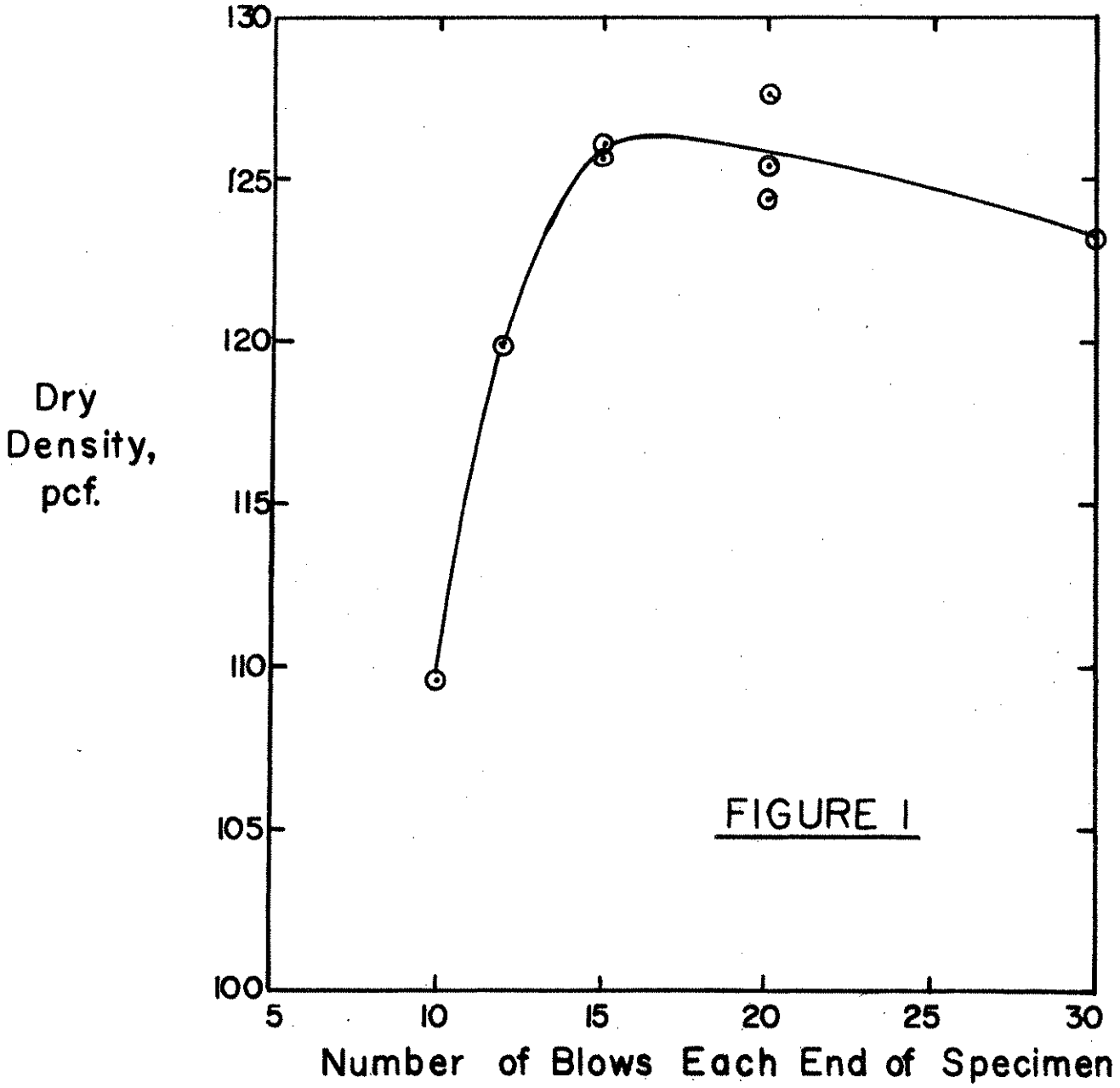
blows on each end of the specimen. The standard dry density could be reasonably reproduced using 15 blows of the hammer on each end of the specimen. At 20 blows on each end of the specimen, the density was much less reproducible. The variation of moisture content following compaction from the initial mix content of 10.9% was very slight with all specimens.

Figure 2 shows the variation of percent particle size versus number of blows on each end of the specimen. Maximum degradation occurred at 15 blows of the hammer, i.e., almost 12% reduction in the amount of gravel with distributed increases in the other size fractions, from 10 to 15 blows on each end of the specimen.

As previously noted, the moisture content of each specimen point in Figs. 1 and 2, both prior to and following molding, was very closely related. Thus there appears to be no reasonable correlation between amount of degradation and number of blows, due to moisture content. Because the degradation is shown to be less at 20 and 30 blows than at 15 blows, but still greater than at 10 blows, it is thought that the higher numbers of blows causes packing of the particles which tends to inhibit increased degradation. Such is further assumed because of the slight reduction of density from 15 to 20 to 30 blows as in Fig. 1.

D. Vibratory Compaction

In the three preceeding sections, the state of compaction relies on either pounding or pushing the particles into an intimate arrangement. Vibratory compaction relies heavily on the proper combinations of frequency, amplitude, amount of time of vibration and amount of surcharge weight on top of the sample to produce the desired state of densification.
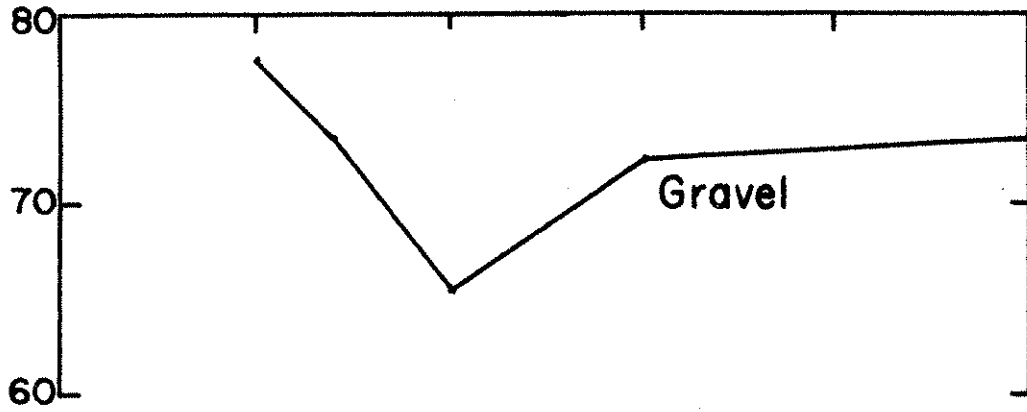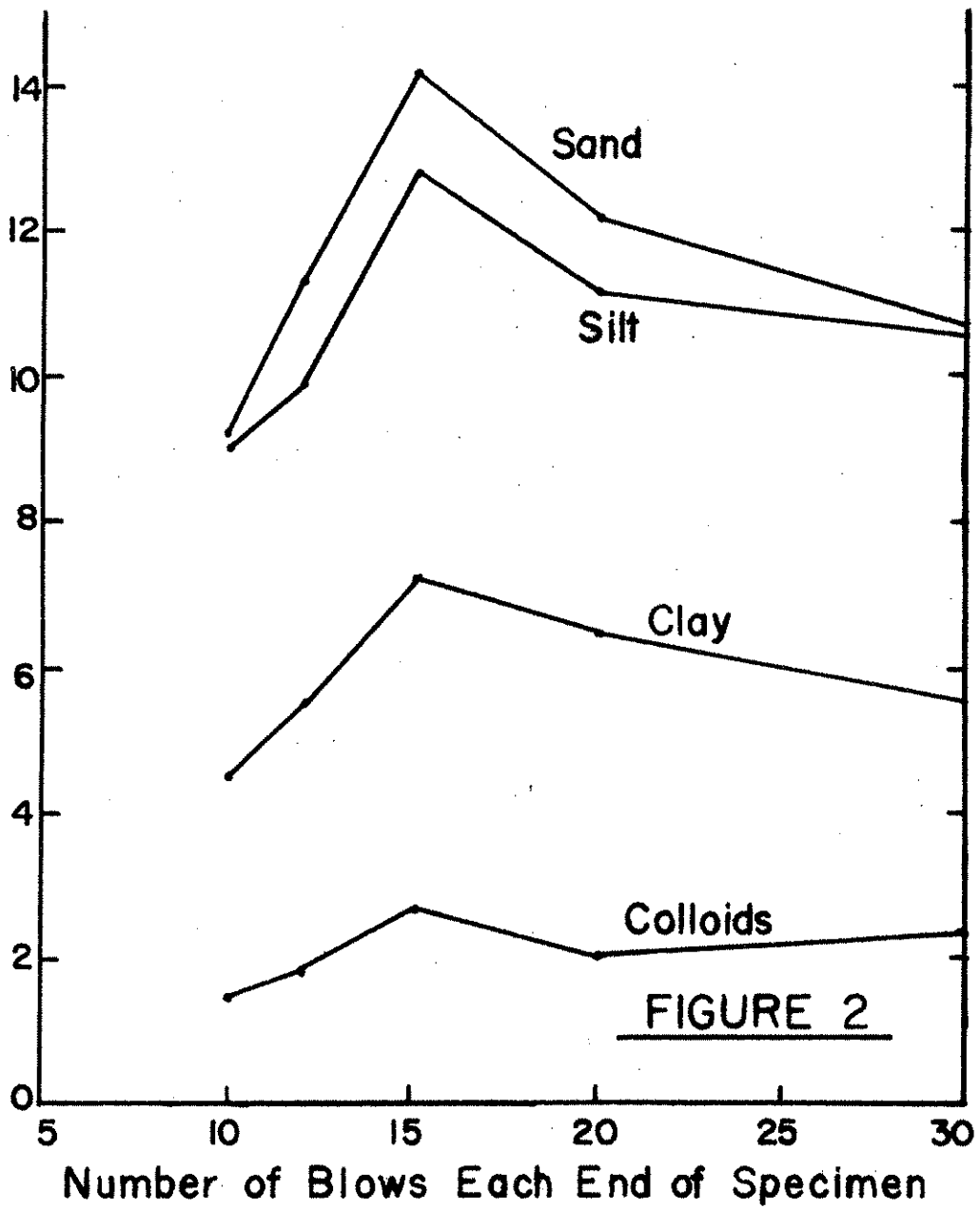
FIGURE 2

In this phase of compaction, the following procedure was used:

1. Sufficient Bedford material, hand mixed to optimum moisture content (10.9%) for maximum standard density (127.4 pcf) in a specially built 1/30-cu ft Proctor mold[*], was weighed, placed in the mold and rodded until refusal.

2. A weight was placed on top of the specimen and vibrated under the conditions noted below.

3. The weight was then removed and the specimen was measured for height.

After the mold was removed from the table each specimen was weighed, extruded and examined for visual segregation. Duplicate moisture content samples were removed from each specimen and the remainder was retained for mechanical analysis.

The frequency of vibration of each specimen was held constant at 3600 cycles per minute on the Syntron Electric Vibrator table. Duplicate specimens were produced for each of the following variables:

1. Vibration periods of 1/2, 1 and 2 minutes.

2. Surcharge weights of 15, 25 and 35 lb.

3. Three settings of amplitude dial, each causing a change of amplitude under the three weights as shown in the following table:

Surcharge weight (lb)	Amplitude control dial setting	Measured amplitude of vibration (mm)
15	10	0.764
	50	0.863
	90	0.915
25	10	0.332
	50	0.705
	90	0.551
35	10	0.330
	50	0.320
	90	0.368

[*]The mold was specially built for attachment to the vibratory table.

Amplitudes were measured by gluing a fine thread to the edge of
the vibrator table, stopping the visible motion of the thread with a strobo-
scope light beam, and measuring the vertical displacement of the thread with
a cathetometer. A minimum of three such readings gave the average values
noted in the above table.

Table 7 summarizes the effect of the vibratory compaction variables on
the particle size degradation. The major vibratory compaction variable was
the surcharge weight on top of the specimen, the greatest amount of
degradation occurring with the 15-lb weight.

Table 7. Effect of vibratory compaction variables on particle size degradation.

Vibratory compaction variable	Average AASHO-ASTM particle size (% of dry sample)				
	Gravel	Sand	Silt	Clay	Colloids
Surcharge weight (lb)					
15	66.4	16.2	11.4	6.0	1.8
25	70.0	14.6	10.1	5.3	1.6
35	73.2	12.2	9.5	5.1	1.6
Amplitude control dial setting					
10	69.1	14.8	10.5	5.6	1.7
50	69.1	14.4	10.6	5.9	1.7
90	71.5	13.4	10.0	5.1	1.6
Time (minutes)					
1/2	70.3	13.9	10.2	5.6	1.7
1	68.9	14.9	10.6	5.6	1.6
2	70.4	14.2	10.1	5.3	1.6
None-uncompacted control sample	73.2	12.9	8.4	5.5	1.7

Little or no degradation appeared with the combination of 35 lb of sur-
charge weight, amplitude control dial setting of 90 (0.368 mm of amplitude)
and 2 minutes vibration time.

Segregation was visually noted to vary primarily in relationship to
surcharge weight. The 15-lb surcharge specimens were segregated throughout
but segregation became slightly more pronounced at the top of the specimen
immediately under the weight. A thick slurry of water and fines oozed out of
the specimen around the 15-lb surcharge and apparently caused the more pro-
nounced effect of segregation of the larger particles at the top of the specimen.
At the opposite extreme, the 35-lb surcharged specimens were quite uniform
in their appearance with no visual segregation.

Following compaction, moisture content and density also appeared to vary
in relation to surcharge weight. The 15-lb surcharged specimens varied from
almost 100% to as low as 87.7% of the average standard or initial mixing
moisture content. Density of these specimens also varied from 88.9% to
almost 100% of the average AASHO-ASTM standard previously noted. The 35-lb
surcharged specimens produced much more controllable density, averaging 97.3%
of the standard. Likewise, the moisture content, following compaction,
averaged 96.8% of the initial (average standard OMC) mixing moisture.

The optimum combination of variables of 35 lb, 90 dial setting
and 2 minutes vibration time was also applied to a special mold for vibratory
compaction of 4-in. diam by 8-in. high cylinders to be used in Problems 2 and
3 of this project. Degradation was again found to be none to minimal.
Visual segregation was found to be nonexistent, with a few exceptions where the
samples had not been properly obtained from the bins and quartered. Moisture

content following molding was consistently about 97% of the standard 10.9% initial mixing moisture content. Density was consistently reproducible within less than 1.0 pcf but still averaged about 2.0 pcf below the standard.

E. Garner and Gilmore Samples

As previously noted, the Bedford sample was the least hard of the three materials and has been shown in the field to be representative of the least stability. It was used as the major sample of the compaction study as noted in the four preceding sections. Only standard AASHO-ASTM and vibratory compaction procedures were compared using the Garner and Gilmore samples. These methods have been noted previously.

The results followed the same general trends as with the Bedford sample with the exception that:

1. Degradation of the Garner and Gilmore samples under standard AASHO-ASTM compaction was not as pronounced as with the Bedford sample, i.e., a maximum of about 4% decrease by dry soil weight in the gravel fraction while almost double this amount in the Bedford.

2. Little or no visual segregation occurred in any of the vibrated Garner samples.

3. Some slight segregation was noticeable in the 15-lb surcharged Gilmore samples.

4. Due to the lower quantity of fines and lack of plasticity (Table 4) in the Gilmore sample, it was difficult to handle the extruded specimens, several of them falling apart upon handling.

5. With each vibratory compaction variable, the density of the Garner and Gilmore specimens were near or above standard AASHO-ASTM values (Table 4). The 35-lb surcharged samples showed more uniform, controllable densities and were consistently about 3 to 4 pcf above the standard. Moisture content following compaction was consistently lower than mix content as with the Bedford sample.

F. Summary

The vibratory compaction procedure was considered to meet the general criteria of a laboratory compaction method producing the most uniform, controllable density while minimizing degradation and segregation of compacted specimens of each of the three materials. The combination of 3600 cycles per minute frequency, 35-lb surcharge weight, 0.368 mm of amplitude and 2 minutes of vibration time was adopted for general use in the other problem areas of the project.

IV. PROBLEM 2 — SHEAR STRENGTH OF UNTREATED GRANULAR MATERIALS

The purpose of this study was to investigate the effect of gradation, density and mineralogical characteristics of the three crushed stone samples while subjected to shear stresses.

Consolidated-undrained triaxial shear tests with total volume change and pore water pressure measurements were conducted on 4-in. diam by 8-in. high specimens, compacted by the vibratory procedure previously summarized. A rate of deformation of 0.01 in. per minute was used throughout the testing. This test was chosen for Problem Areas 2 and 3 as it more closely duplicates field conditions than other conventional tests, and also allows determination of the various shear strength parameters from one basic test method.

A. Effect of Frictional Interaction and Geometric Constraints

This portion of the problem area evaluated the effect of frictional interaction between particles and the effect of geometric constraints among these particles on the shear strength of the granular materials. Three steps were followed:

1. Development of a theory allowing separate consideration of the two mechanisms.

2. Testing of the theory against available published data on various granular materials.

3. Study of the shear strength and deformational behavior of the three crushed limestones in light of the proposed theory.

Reference is made to Tinoco and Handy[1] for a detailed analysis of this portion

of the problem area.

Based upon energy considerations utilizing triaxial compression tests, the basic equation developed by Tinoco is:

$$\frac{\sigma_1'}{\sigma_3'} = \tan^2 (45 + 1/2\varphi_s) + \frac{\delta v}{\delta \epsilon_1} \tan^2 (45 + 1/2\varphi_s) + \vartheta_D \quad (1)$$

where σ_1'/σ_3' is the ratio of major to minor effective principle stresses at any stage during the deformation process; δv is the increment in natural volumetric strain, being positive when the volume of the sample is increasing; $\delta \epsilon_1$ is the increment in natural axial strain; φ_s is Coulomb's angle of solid friction and ϑ_D is a parameter defined in subsequent paragraphs.

Consider a perfectly plastic and frictional rigid body shearing at no volume change rate. The ratio of major to minor effective principle stresses is given by:

$$\frac{\sigma_1'}{\sigma_3'} = \tan^2 (45 + \frac{\varphi_s}{2}) \quad (2a)$$

Consider a particle assembly shearing at no volume change rate. Then the ratio of major to minor effective principal stresses becomes:

$$\frac{\sigma_1'}{\sigma_3'} = \tan^2 (45 + \frac{\varphi_s}{2}) + \vartheta_D \quad (2b)$$

where the first term of the right side of Eq. (2b) represents the frictional resistance of the assembly considered as a rigid body and ϑ_D represents the shear resistance of a frictionless particle assembly, which is entirely due to the particles rearranging within the assembly.

If the particle assembly is shearing at a given volume change rate at a given instant during the deformation process, then the σ_1'/σ_3' at that

given instant is:

$$\frac{\sigma_1'}{\sigma_3'} = \tan^2 (45 + \frac{\varphi_s}{2}) + \frac{\delta v}{\delta \epsilon_1} \tan^2 (45 + \frac{\varphi_s}{2}) + \mathcal{J}_D \qquad (3)$$

Thus, $\mathcal{J}_D$ is a term representing the required σ_1'/σ_3' ratio to rearrange frictionless particles within the assembly. However, the particles of the assembly are indeed frictional particles and therefore Eq. (1) must be rewritten as

$$\frac{\sigma_1'}{\sigma_3'} = \tan^2 (45 + \frac{\varphi_s}{2}) + \frac{\delta v}{\delta \epsilon_1} \tan^2 (45 + \frac{\varphi_s}{2}) + \mathcal{J} + \mathcal{J}_f \qquad (4)$$

The term $\mathcal{J}$ is that part of the σ_1'/σ_3' ratio spent in rearranging the particles as if they were frictionless. The $\mathcal{J}_f$ is that part of the σ_1'/σ_3' ratio spent in rearranging the particles considered as possessing friction.

Thus, the strength of a particle assembly is considered first as the strength of a rigid body; second, it is considered an ideal frictionless particle assembly which led to Eq. (2b); third, the rigid body is considered to change in volume when it is sheared as a result of which Eq. (1) is obtained; and fourth, the ideal frictionless particle assembly is transformed into a frictional particle assembly which leads to Eq. (4).

The values of σ_1'/σ_3' and $\delta v/\delta \epsilon$ are known at any stage of the deformation process during the triaxial compression test. Thus, Eq. (1) involves two unknowns, φ_s and $\mathcal{J}_D$.

Before proceeding toward the solution for φ_s and $\mathcal{J}_D$, it is convenient to rearrange Eq. (1) in order to obtain the following:

$$\frac{\sigma_1'}{\sigma_3'} - (1 + \frac{\delta v}{\delta \epsilon_1}) = \mathcal{J} + [\frac{\sigma_1'}{\sigma_3'} + (1 + \frac{\delta v}{\delta \epsilon_1})] \sin \varphi_s \qquad (5)$$

Experimental data obtained from the triaxial test shows Eq. (5) to be plotted as $\sigma_1'/\sigma_3' - (1 + \delta v/\delta \epsilon_1)$ versus $\sigma_1'/\sigma_3' + (1 + \delta v/\delta \epsilon_1)$. If this plot becomes a straight line over a wide range of deformation, then it is possible to determine the values of φ_s and ϑ_D. If the plot is not a straight line over a wide range of deformation, then independent determination of φ_s and ϑ_D is not possible.

There are no reasons to assume that ϑ_D will indeed be a constant during a given range of the deformation process. However, the above statement leads to two alternatives in the case that the plot does not become a straight line: (a) Independent determination of φ_s and ϑ_D is not possible; or (b) the experimental evaluation of the term $\delta v/\delta \epsilon_1$ is not correct. The value of φ_s depends on the nature of the mineral, the properties of its surface and the size of the load per particle[2]. The parameter ϑ_D is a function of the packing characteristics of the assembly and is therefore dependent upon gradation, particle arrangement, particle size, stress history and type of shear test[1].

Once the value of φ_s is determined, the value of ϑ may be determined at any stage of the deformation process. With ϑ known at any stage of deformation, the following quantities may be readily determined:

$$\frac{\delta W_{iD}}{\sigma_3' \delta \epsilon_1} = \frac{\delta v}{\delta \epsilon_1} + \frac{\vartheta}{1 - \sin \phi_s} \tag{6a}$$

$$\frac{\delta W_{if}}{\sigma_3' \delta \epsilon_1} = (\frac{\sigma_1'}{\sigma_3'} - 1) - \frac{\delta W_{iD}}{\sigma_3' \delta \epsilon_1} \tag{6b}$$

$$\vartheta_D = \frac{\vartheta}{1 - \sin \phi_s} \tag{6c}$$

$$\vartheta_f = \frac{\vartheta}{1 - \sin \phi_s} - \vartheta \tag{6d}$$

where δW_{iD} and δW_{if} are the increments in the rate of internal work absorbed

in dilatancy and friction, respectively. The terms $\delta W_{iD}/\sigma_3' \delta \epsilon_1$ and

$\delta W_{if}/\sigma_3' \delta \epsilon_1$ are the ratios of the increments in the rate of internal work

absorbed in dilatancy or friction to the product of the minor effective principal

stress by the increments in natural axial strain. The terms $\delta W_{iD}/\sigma_3' \delta \epsilon_1$ and

$\delta W_{if}/\sigma_3' \delta \epsilon_1$ do not represent a particular energy ratio but are selected for

convenience and simplicity of calculation.

In the following section of this report let

$$\frac{\delta W_{if}}{\sigma_3' \delta \epsilon_1} = F, \quad \frac{\delta W_{if}}{\sigma_3' \delta \epsilon_1} + \mathcal{G}_f = F', \quad \text{and} \quad \frac{\delta W_{if}}{\sigma_3' \delta \epsilon_1} + \mathcal{G}_f + \mathcal{J} = D \quad (7a,b,c)$$

1. Determination of the Angle of Solid Friction of the Crushed Limestones

Determination of the angle of solid friction was made from Eq.(5). The

term $\delta v/\delta \epsilon_1$ is the ratio of the increment in natural volumetric strain to

the natural axial strain. However, the data used in this project gives v

in terms of the initial volume and the axial strain in terms of the initial

length of the tested specimen. Thus v and ϵ_1 represent the "engineering"

volumetric strain and the "engineering" axial strain. Therefore it is assumed

that the ratio of the increment in natural volumetric strain to the increment

in natural axial strain is approximately equal to the ratio of the increment

in "engineering" volumetric strain to the increment in "engineering" axial

strain; the notation used for the latter is the same as the one used for the
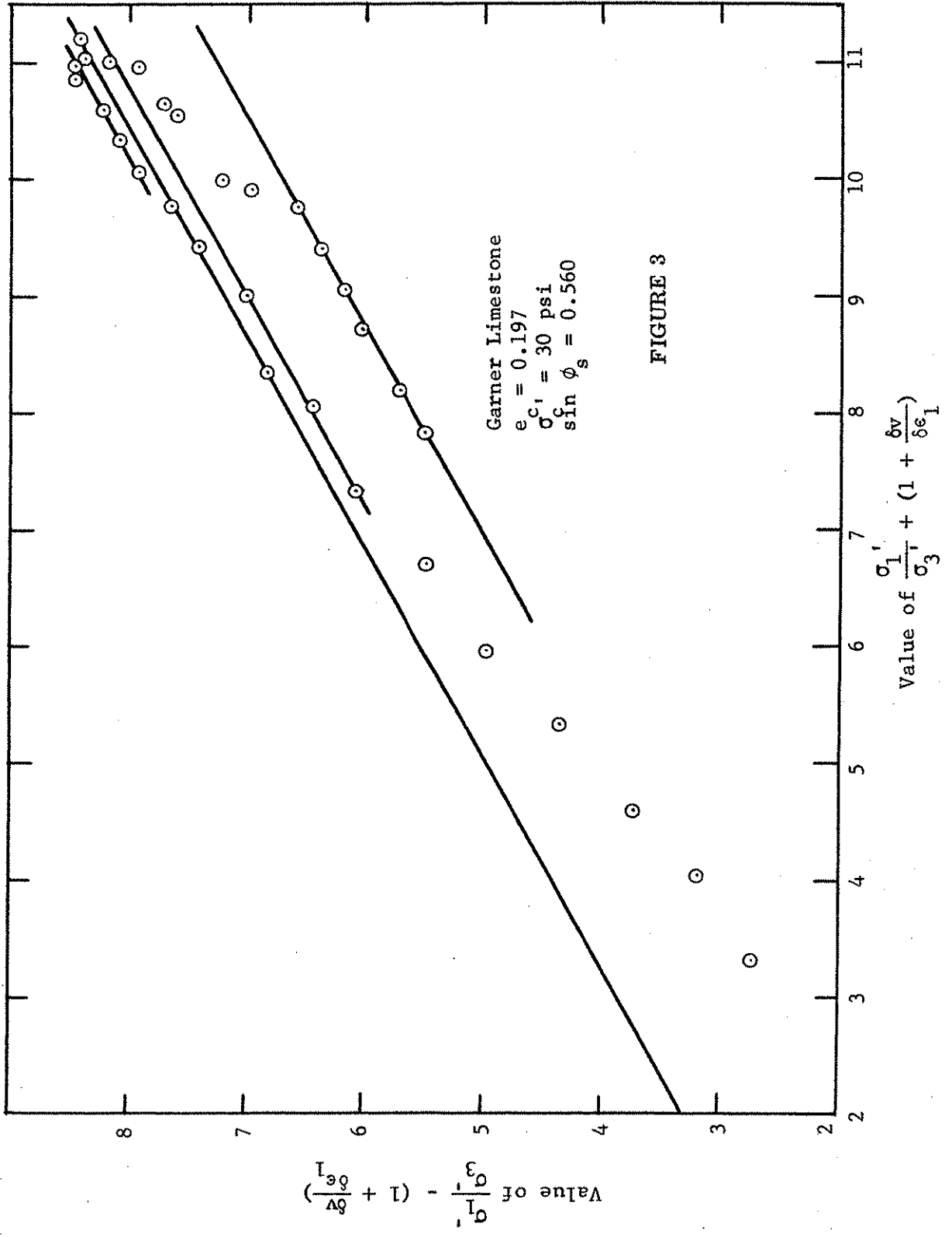
former.

Equation (5) was applied to selected results from the numerous triaxial

tests performed. The selection was based on variables which may have had an

influence on the behavior of the crushed limestones such as void ratio, level

of confining pressure, stress history and change in sample gradation.

Figures 3 through 6 illustrate four of the selected plots of Eq. (5).
Linear relations were found over a wide deformation range regardless of the
variables being investigated. Two features common to most of the plots were
the existence of more than one linear relation, and deviation from a linear
relation during the initial stages of deformation (less than one percent of
the axial strain). Existence of more than one linear relation may be due to
the use of "fixed" ends, which introduce nonuniformity of strains within
the specimen.

Calculated values of $\sin \varphi_s$ ranged from 0.560 to 0.565, respectively,
corresponding to solid friction angles of 34.1° to 34.4° for the three
stones. The average value of the angle of solid friction for the crushed
limestones was 34.2°, indicating that the method allows the calculation of
φ_s which is solely dependent on the mineralogical characteristics of the
particles. Calcite was the predominant mineral found in each of the lime-
stone samples. Horn[3] performed tests on pure calcite and obtained an
angle of friction of 34.2° under submerged conditions.

Figure 4 illustrates a reloading test with the Gilmore stone. This
specimen was unloaded after the maximum value of σ_1'/σ_3' was reached, and again
loaded to maximum σ_1'/σ_3'. No significant changes were produced in the plot.
The calculated value of $\sin \varphi_s$ is 0.562 for a solid friction angle of 34.2°.

Triaxial tests performed on the crushed limestones revealed that the
values of the parameter ϑ were functions of the confining pressure and the
stage of deformation at which the measurement was made. This indicates that
ϑ is not only a function of the gradation but a function of particle arrange-
ment in the case of well-graded granular materials, as is the case of the

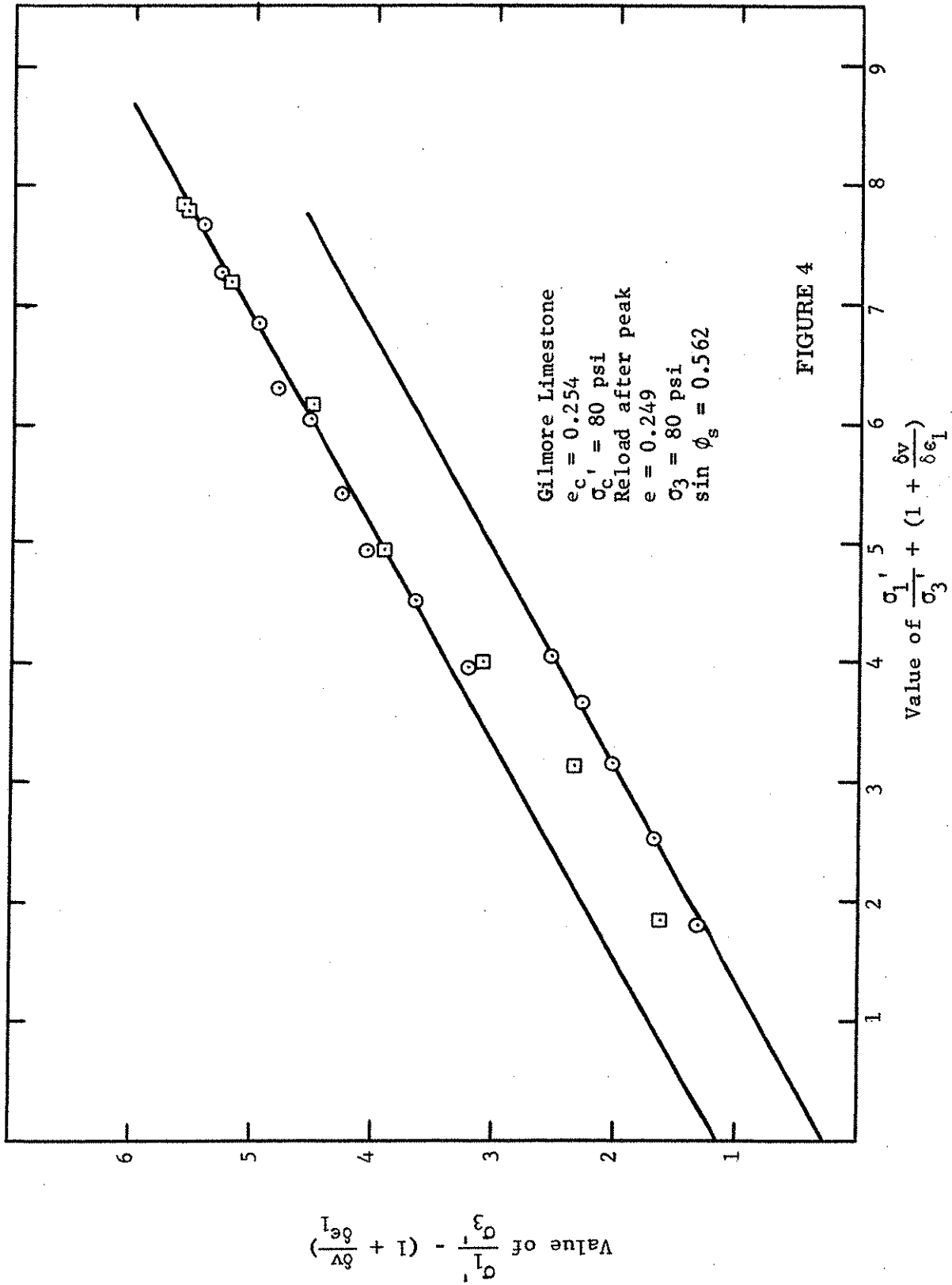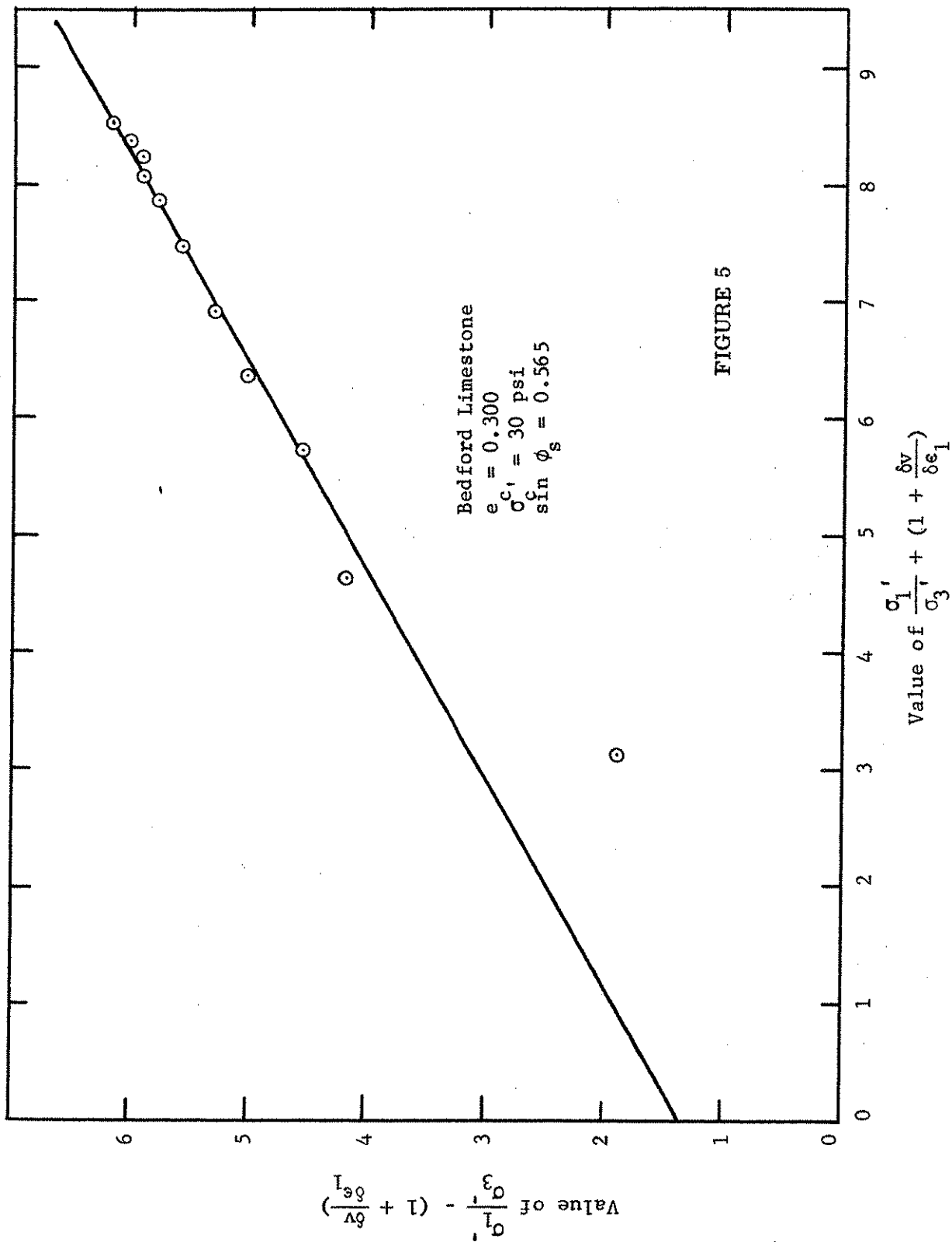Garner Limestone
$e_c = 0.197$
$\sigma_3' = 30$ psi
$\sin \phi_s = 0.560$

FIGURE 3

Value of $\frac{\sigma_1'}{\sigma_3'} + (1 + \frac{\delta v}{\delta \epsilon_1})$

Value of $\frac{\sigma_1'}{\sigma_3'} - (1 + \frac{\delta v}{\delta \epsilon_1})$

Gilmore Limestone
$e_c = 0.254$
$\sigma_c' = 80$ psi
Reload after peak
$e = 0.249$
$\sigma_3 = 80$ psi
$\sin \phi_s = 0.562$

Value of $\frac{\sigma_1'}{\sigma_3'} + (1 + \frac{\delta v}{\delta \epsilon_1})$

Value of $\frac{\sigma_1'}{\sigma_3'} - (1 + \frac{\delta v}{\delta \epsilon_1})$

FIGURE 4

Bedford Limestone
$e_c = 0.300$
$\sigma_3^{c'} = 30$ psi
$\sin \phi_s = 0.565$

FIGURE 5

Value of $\dfrac{\sigma_1'}{\sigma_3'} + (1 + \dfrac{\delta v}{\delta \epsilon_1})$

Value of $\dfrac{\sigma_1'}{\sigma_3'} - (1 + \dfrac{\delta v}{\delta \epsilon_1})$

Bedford Limestone
Retained on No. 200 sieve
$e_c = 0.265$
$\sigma_c' = 30$ psi
$\sin \phi_s = 0.563$

Value of $\dfrac{\sigma_1'}{\sigma_3'} + (1 + \dfrac{\delta v}{\delta \epsilon_1})$

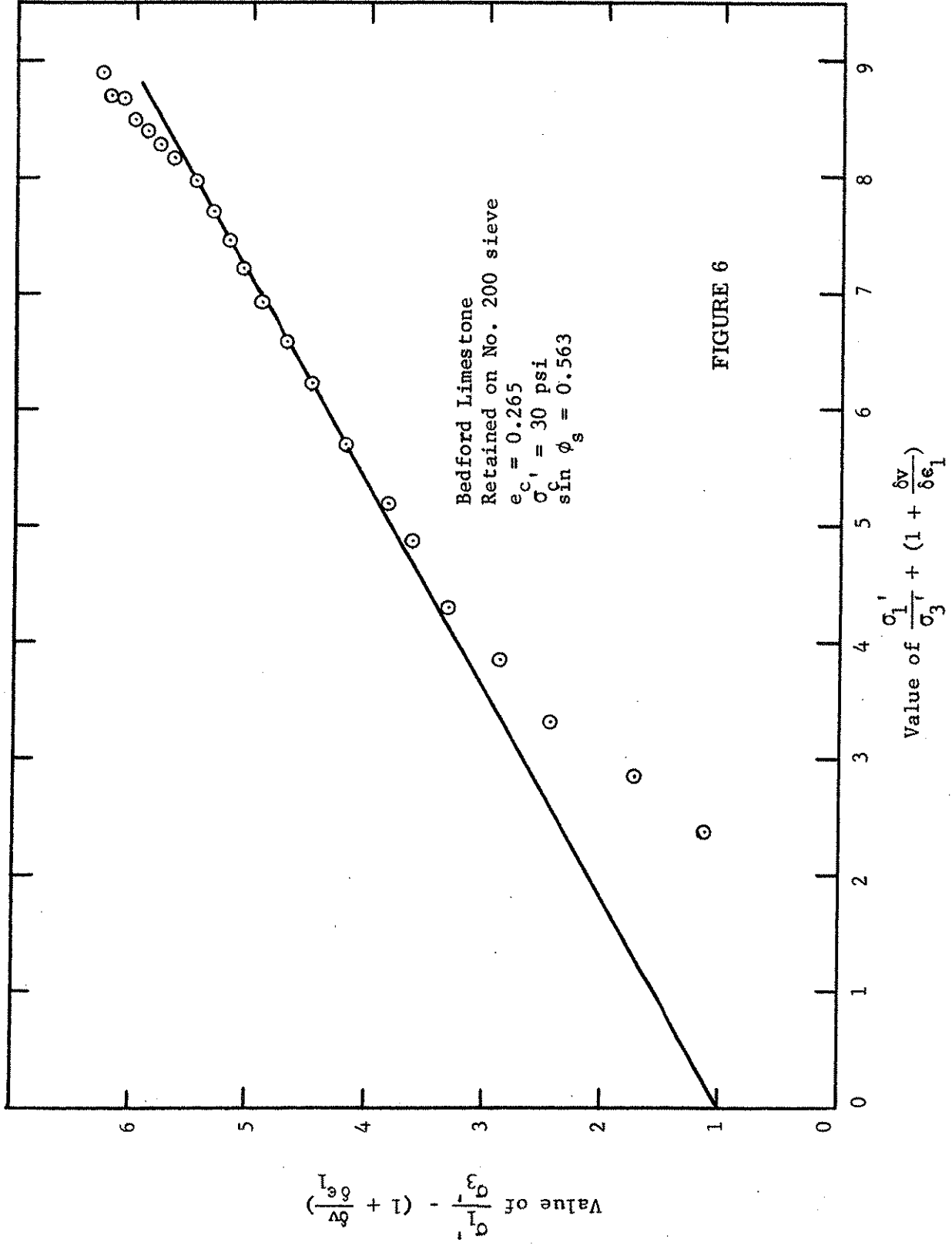Value of $\dfrac{\sigma_1'}{\sigma_3'} - (1 + \dfrac{\delta v}{\delta \epsilon_1})$

FIGURE 6

crushed limestones used herein. Because the value of ϑ changes with changes
in deformation, it was not possible to assign unique values of ϑ for a given
material. Therefore, the usefulness of this parameter was in the calculation
of the functions F, F' and D which describe the behavior of the specimen
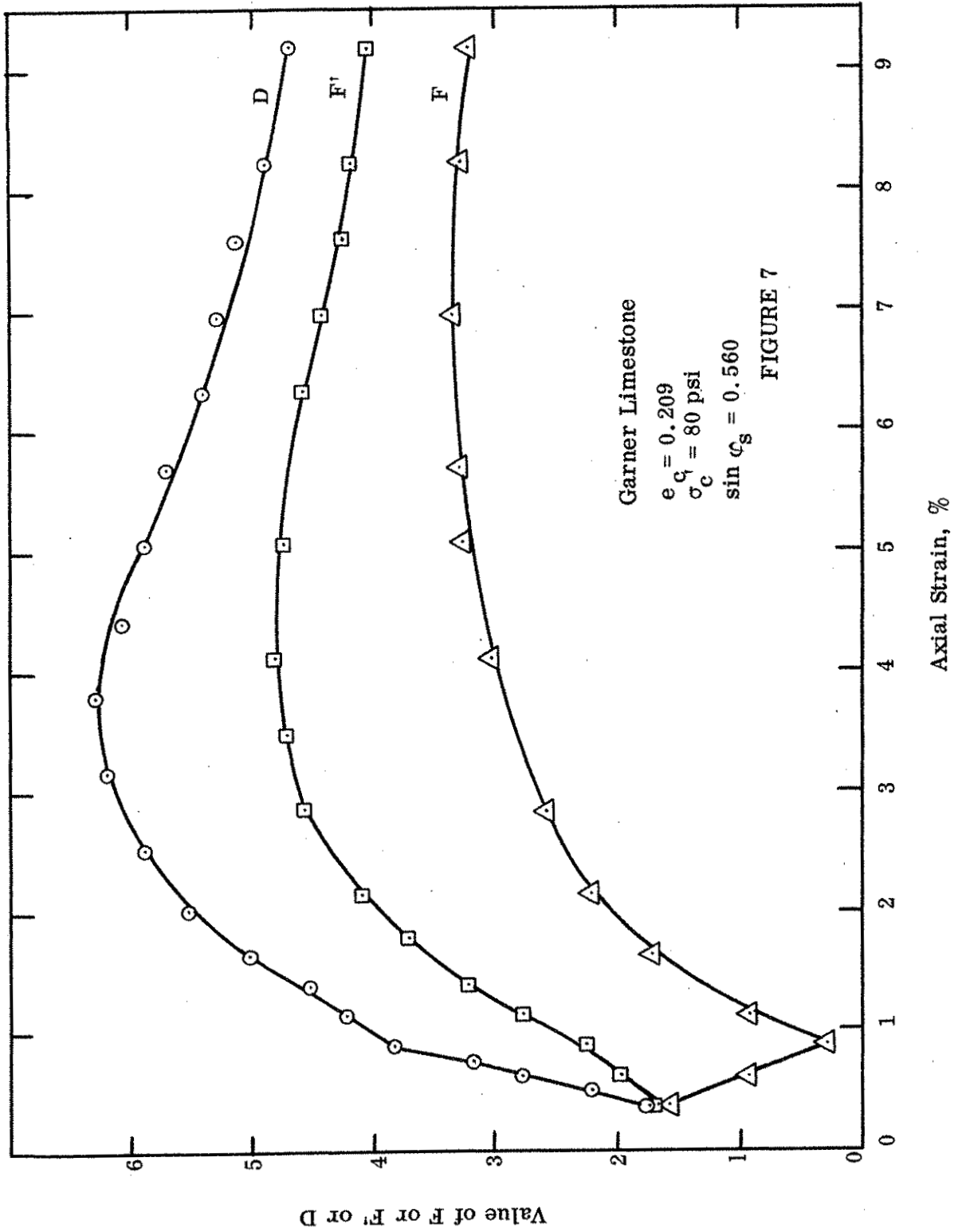during deformation.

2. Significance of the Functions F, F', and D

Figures 7 to 13 show plots of the functions F, F' and D versus the
"engineering" axial strain in percent.

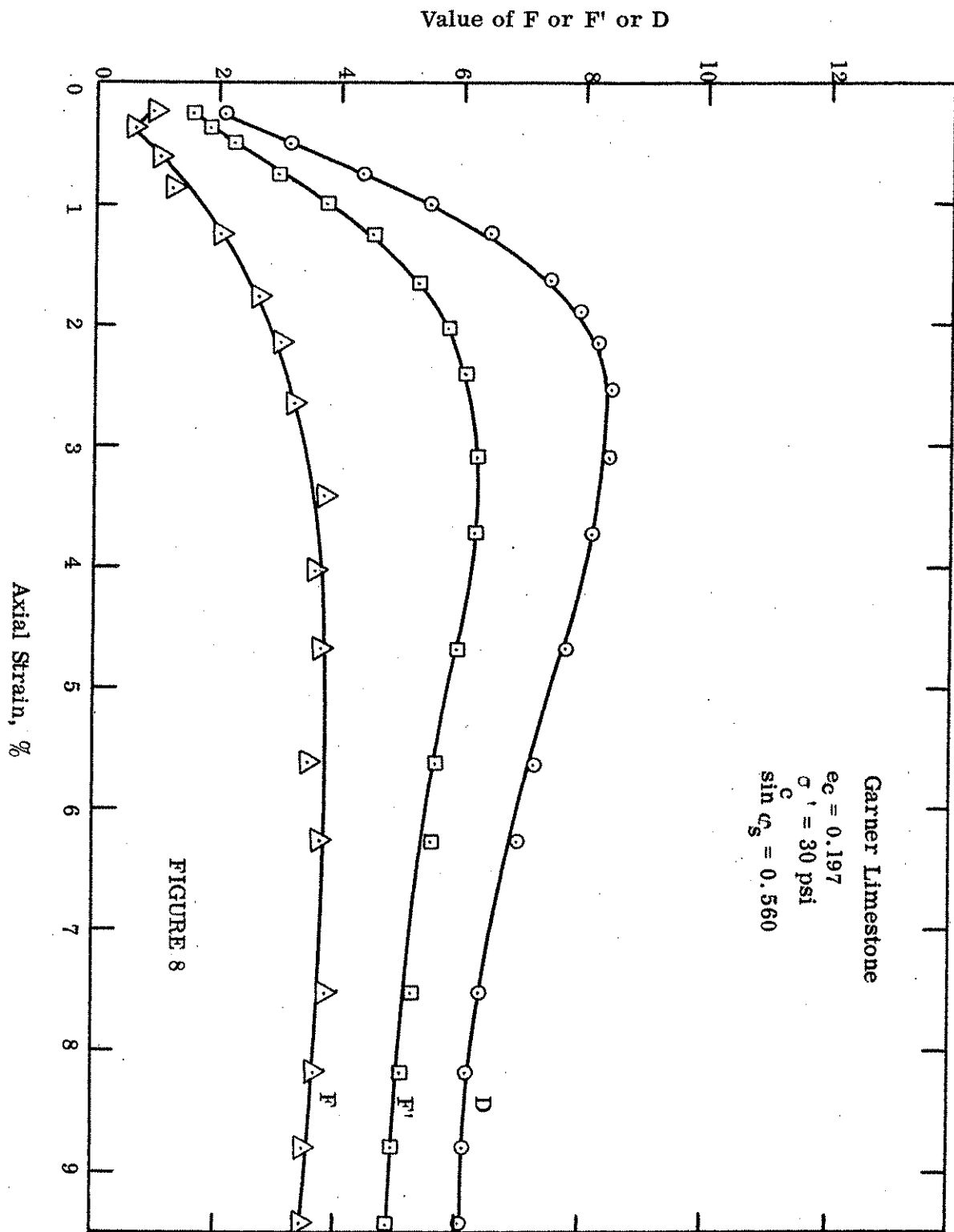Function F represents the rate at which friction is developed within the
sample. Thus, a plot of the function F versus the axial strain represents
the changes in the rates at which friction is developed within the sample
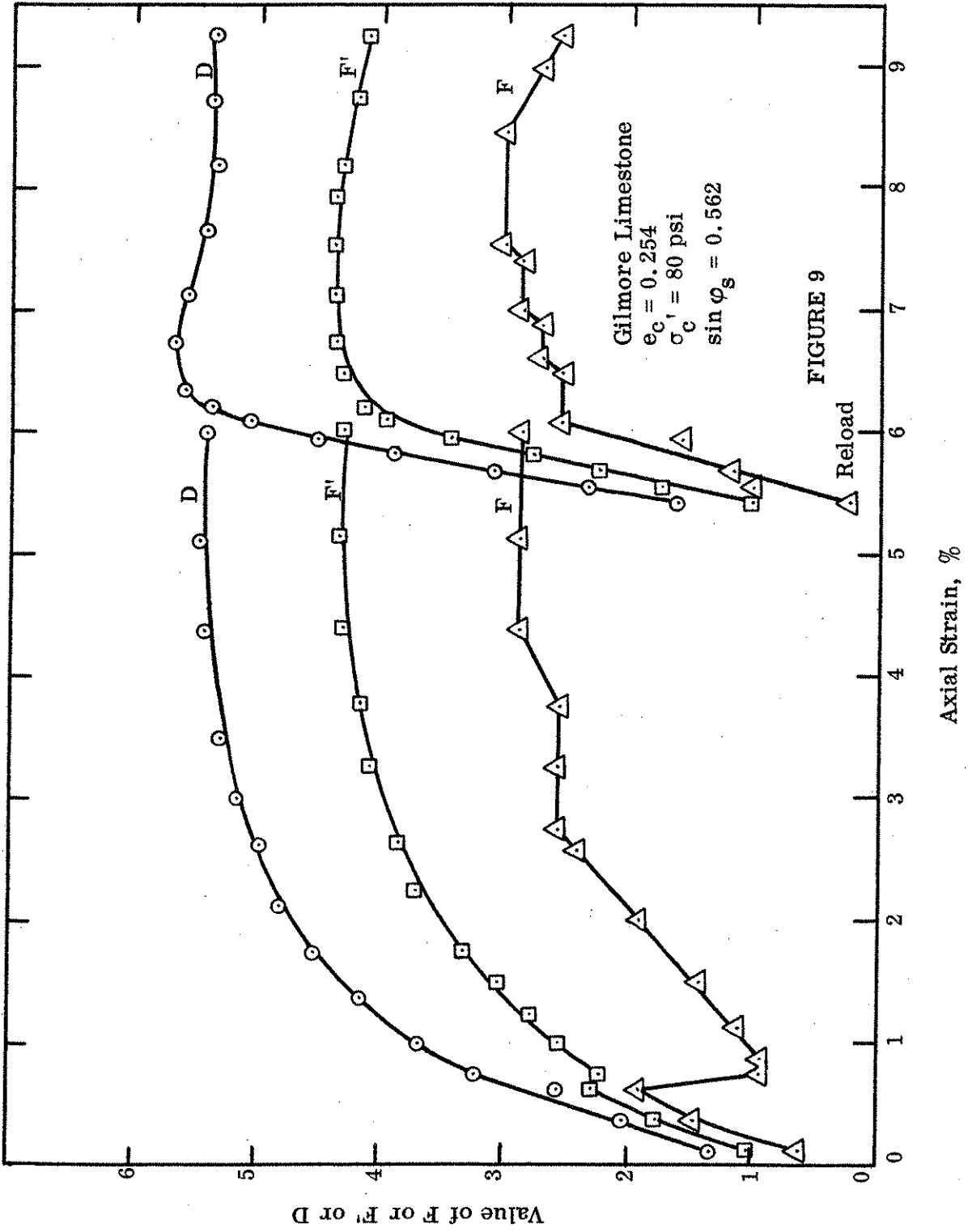as the test progresses.

Figures 7 and 8 represent the above plot for Garner limestone tested
at confining pressures of 80 and 30 psi respectively. Comparison of the
development of the function F between the figures emphasizes effect of the
confining pressure in the deformational behavior of the samples.

Figure 7 shows a decrease in the rate of frictional development during
the initial stages of deformation. This behavior suggests weak groups of
particles are rearranged producing a compaction or densification process
within the sample. After this initial stage is overcome, there is gradual
increase in rate of frictional development. From Fig. 8, densification of
the sample tested at a confining pressure of 30 psi takes place rather
immediately.

Thus, the effect of higher confining pressures is to increase the pheno-
menon of rolling between particles or group of particles, usually associated
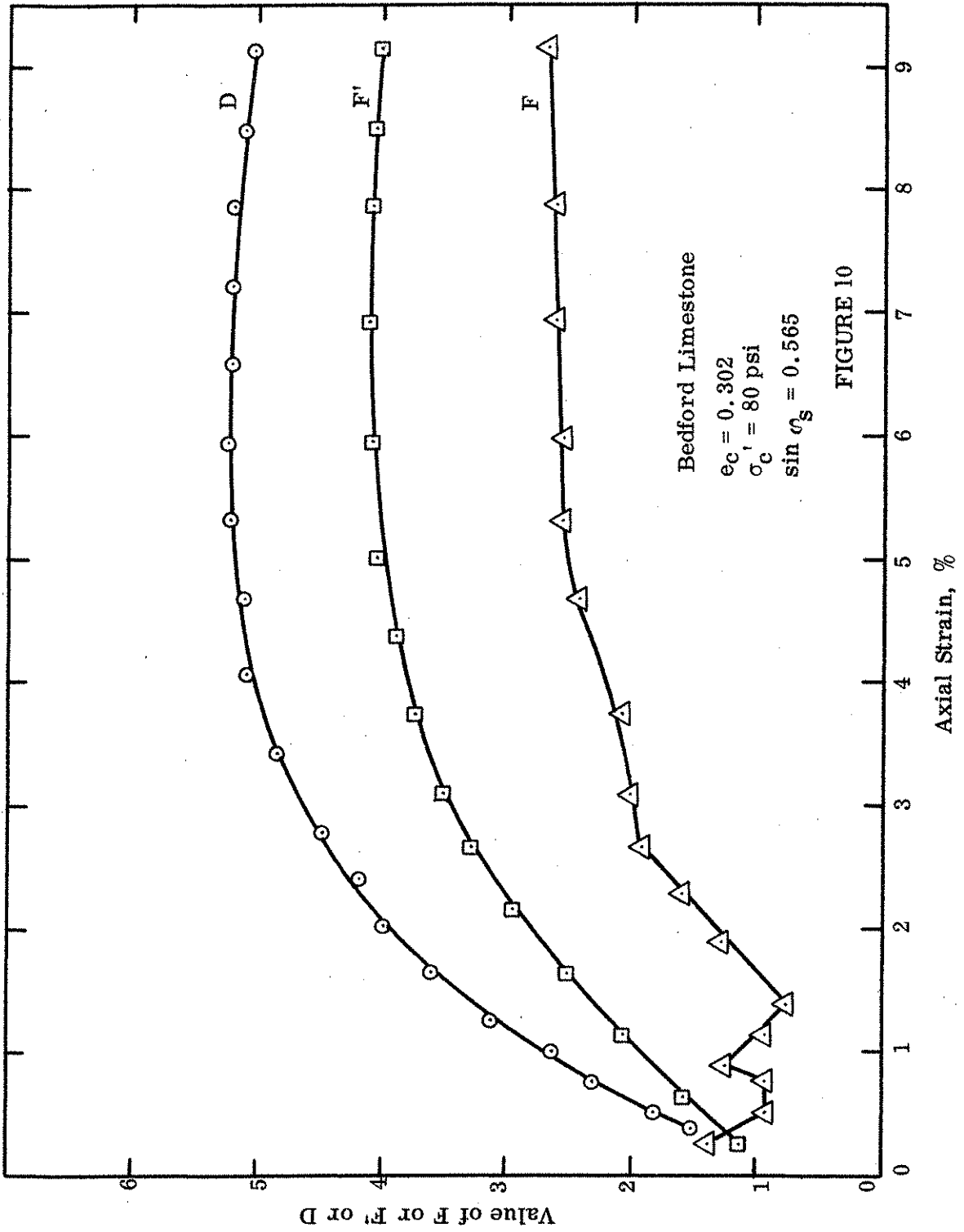with volume decreases within the sample. This means that the process of

Garner Limestone

$e_c = 0.209$

$\sigma_c = 80$ psi

$\sin \phi_s = 0.560$

FIGURE 7

Axial Strain, %

Value of F or F' or D

FIGURE 8

Garner Limestone

$e_c = 0.197$

$\sigma'_c = 30$ psi

$\sin c_s = 0.560$

Value of F or F' or D

Axial Strain, %

Gilmore Limestone
$e_c = 0.254$
$\sigma_c' = 80$ psi
$\sin \varphi_s = 0.562$

FIGURE 9

Axial Strain, %

Value of F or F' or D

Bedford Limestone

$e_c = 0.302$

$\sigma_c' = 80$ psi

$\sin \sigma_s = 0.565$

FIGURE 10

Axial Strain, %

Value of F or F' or D

34

Bedford Limestone
$e_c = 0.266$
$\sigma_c^i = 80$ psi
$\sin \varphi_s = 0.565$

FIGURE 11

Axial Strain, %

Value of F or F' or D

Bedford Limestone

$e_c = 0.300$

$\sigma_c' = 30$ psi

$\sin \varphi_s = 0.565$

Axial Strain, %

Value of F or F' or D

FIGURE 12

Bedford Limestone
Retained on No. 200 sieve

$e_{c'} = 0.265$
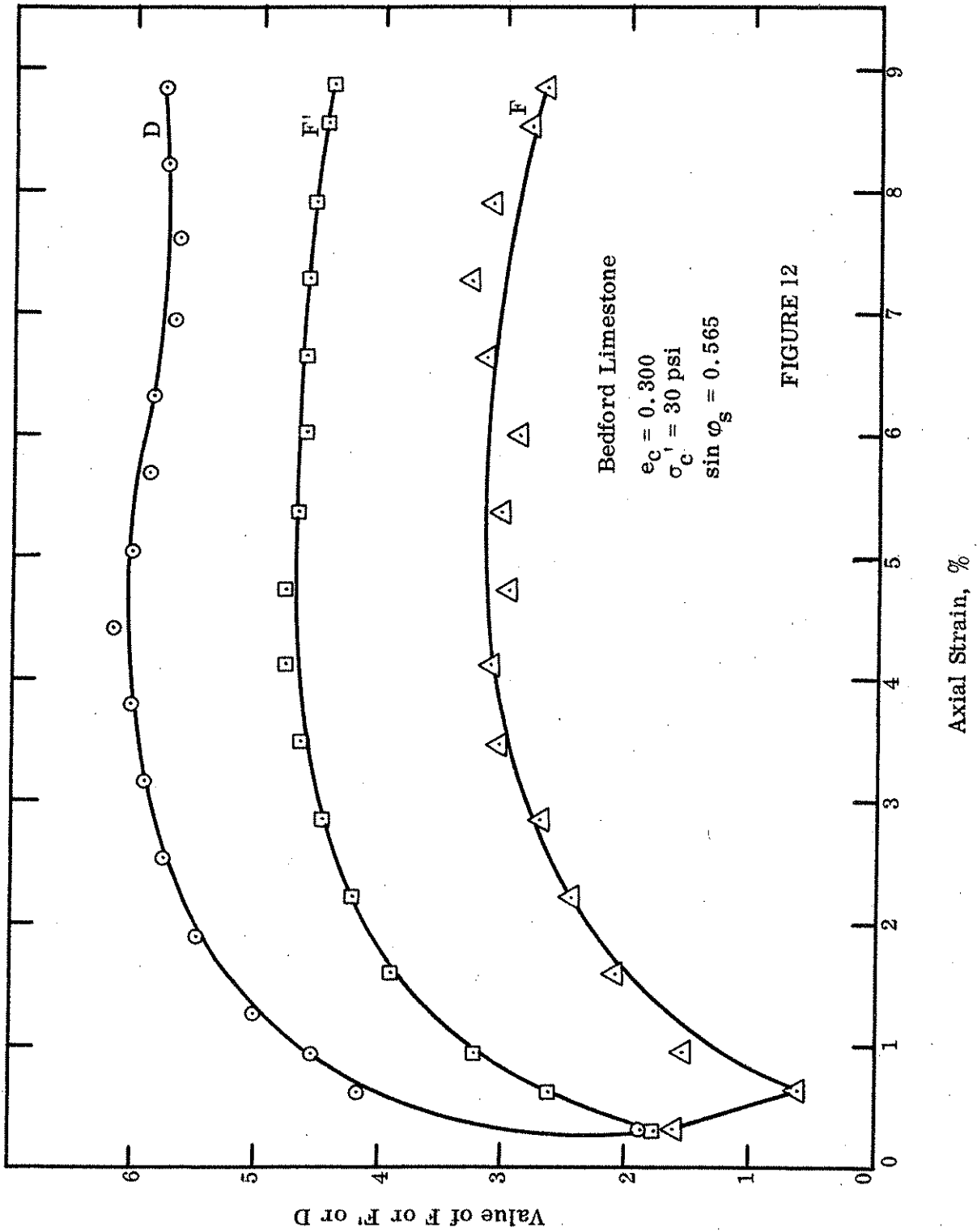$\sigma_{c}' = 30$ psi
$\sin \phi_{s} = 0.563$

FIGURE 13

Axial Strain, %

Value of F or F' or D
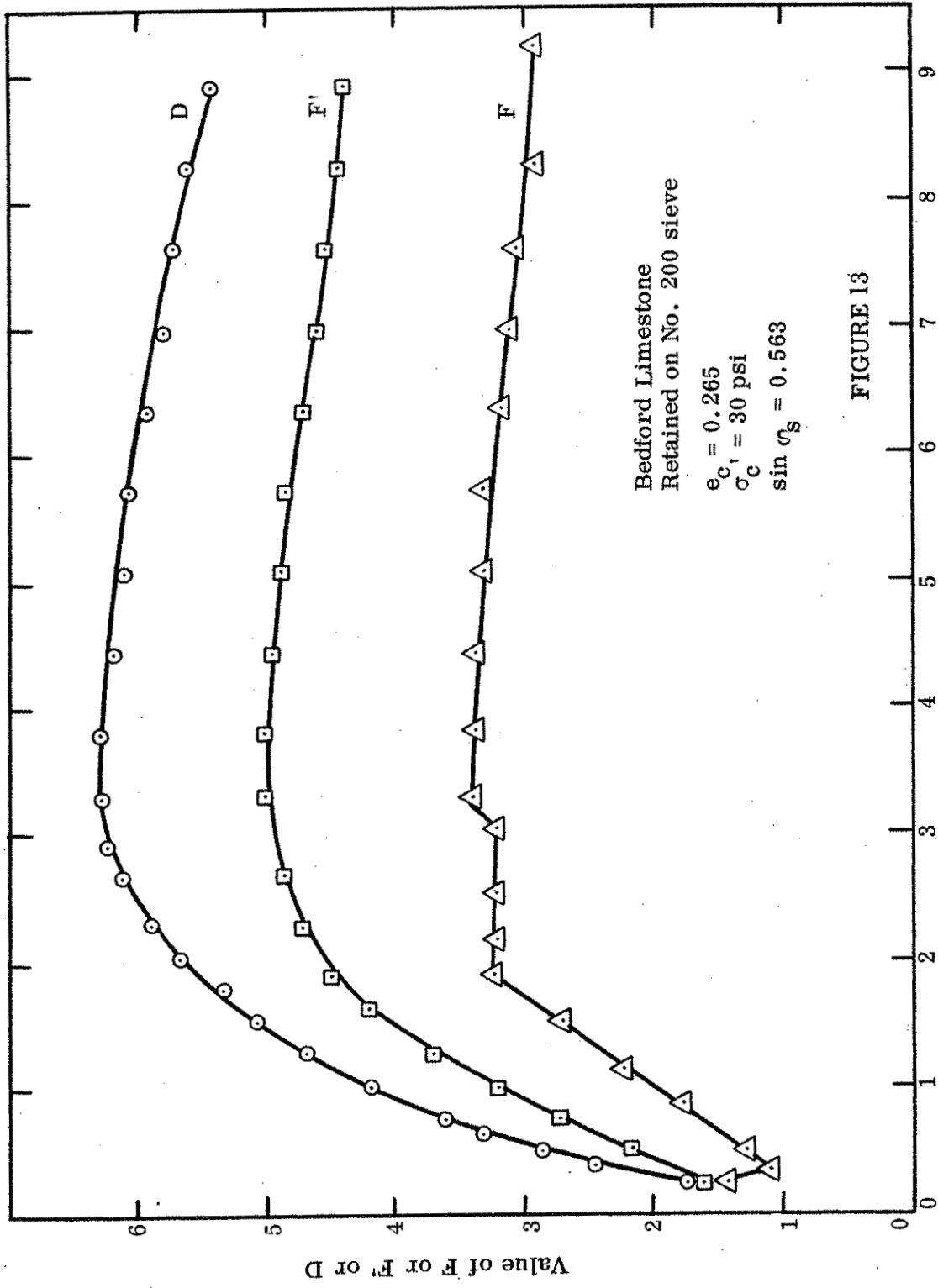
deformation of the granular sample is different under different confining pressures. The rearrangement of the particles caused by rolling under high confining pressures, for example 80 psi, must be reduced if a second loading or a reloading is applied to the sample after the initial stage of densification is overcome. This is clearly seen in Fig. 9 for a Gilmore sample tested at a confining pressure of 80 psi, initially loaded to the maximum value of σ_1'/σ_3', unloaded and again loaded to the maximum value of σ_1'/σ_3'.

It may be argued that slight differences in initial void ratio between the Garner samples at 80 and 30 psi (Figs. 7 and 8) was the cause of the differences in behavior presented above. However, similar phenomenon occurred between samples of the Bedford limestone tested at 80 and 30 psi and at about the same initial void ratio.

Function F' represents the combined effect of friction and particle rearrangement due to friction. The term "particle rearrangement due to friction" requires a brief explanation. A granular system, when sheared, changes its volume. The volume change is not only reflected by the change in position of individual or a group of particles, but also produces additional work absorbed in friction to enable the particle or group of particles to change their relative positions with each other. The calculation of parameters ϑ and ϑ_f was directed to separate these two effects, namely, the work done in changing the sample volume and the additional work done in friction due to this volume change within the sample. This separation of effects is thought to be the clue for obtaining an angle of solid friction which is solely dependent upon the mineralogical characteristics of the particles.

The plot of F' versus axial strain represents the changes in rates at

which total friction is developed within the sample. Total friction is understood to be the combined effect of sliding friction and the additional work done in friction due to particle rearrangement.

Effect of confining pressures again show in the rate of development of F' with respect to axial strain. However, there is a faster rate of decrease in the development of F' in a sample tested at a confining pressure of 30 psi than in a sample tested at 80 psi after the maximum value of σ_1'/σ_3' has been reached. This indicates a more "unstable" structure in the sample at 30 psi after the maximum value of σ_1'/σ_3' is reached. This may be expected because maximum potential energy within the particle assembly is easily reached at lower confining pressures.

Function D represents the combined effect of friction due to sliding, plus particle rearrangement due to friction, plus particle rearrangement due to changes in the volume of the sample. Function D represents, at any given instant in the deformation process, the rate at which the total internal work, after being corrected for volume change, is developed within the sample. Thus, the plot of the function D versus the axial strain represents changes in the rate of total internal work after being corrected for volume changes developed within the sample as the test progresses.

The only significant difference in the development of function D between samples tested at 80 and 30 psi is the change in curvature exhibited by the former during initial stages of deformation and due to densification taking place at this early stage of deformation.

The initial process of compaction will render a modulus of deformation which increases with the confining pressure, where the modulus of deformation is the ratio of $\sigma_1'-\sigma_3'$ to the required axial strain.

Shape of the curves indicates that the maximum value of σ_1'/σ_3' is reached

at lower axial strain for samples at lower than for samples at higher confining

pressures. The difference in axial strain may be explained on the basis that

the greater deformation required for the latter is due to the process of

densification taking place during the initial stages of the deformation process.

3. Comparison of Deformation Characteristics of the Three Crushed Limestones

Effect of void ratio on the values of F, F' and D for Bedford limestone

samples tested at a confining pressure of 80 psi is shown in Figs. 10 and 11.

The higher void ratio specimen (Fig. 10) shows a very slow development of the

function F as the test progresses, indicating a densification process which

in time results in a very slow frictional development. The sample at lower

initial void ratio (Fig. 11) develops friction at a much faster rate. In

fact, the rate of development of the functions F, F' and D are each faster

at lower initial void ratio. The maximum value of σ_1'/σ_3' is the same for

both samples in spite of the differences in initial void ratio. If the

maximum value of σ_1'/σ_3' is chosen as the strength criteria to evaluate these

two samples, then no difference in behavior of the two is found. However,

if a closer inspection is made of the difference between the values of D and

F, such difference is much larger for the sample at high initial void ratio

than for the lower initial void ratio sample. In fact $\delta W_{iD}/\delta W_{if}$ for both

samples are 1.00 and 0.69, respectively. Thus, even if the maximum value

of σ_1'/σ_3' is the same for both samples, there is a difference in the composition

of their strength. The sample at higher initial void ratio achieves this ratio

because a greater amount of work is spent in dilation and indicates that it re-

quired larger amounts of strain to develop the same value of σ_1'/σ_3'. This indicates

that the mechanism of deformation of this sample under the applied loads
consists mainly of rearrangement of particles due to rolling, whereas the
mechanism of deformation of the sample at a lower void ratio consists mainly
of sliding of the particles.

The number of sliding contacts within the sample at lower void ratio is
greater than the sample at higher initial void ratio. However, the number
of sliding contacts available within a given sample is not directly related to
the initial void ratio since the latter is not completely representative of
the packing characteristic of the sample. Definition of a sliding contact
in a particle assembly is presented in Reference 1.

Comparison of the Garner and Bedford limestones tested at a confining
pressure of 80 psi can be made from Figs. 7 and 11. Rate of development of
function F for both samples is about the same. There are marked differences
in the rate of development of functions F' and D, indicating that the strength
measured by the maximum value of σ_1'/σ_3' is also markedly different.

If rate of development of function F (Figs. 7 and 11) is directly related
to the relative number of sliding contacts within the sample, then, in spite
of the difference in initial void ratio, the relative number of sliding
contacts is about the same for both samples. Differences in amount of
deformation required to reach maximum F are due to the densification taking
place within the Garner sample during the initial stage of deformation. Again,
there is a large difference between the ratio $\delta W_{iD}/\delta W_{if}$ for both samples.
Values of the ratio $\delta W_{iD}/\delta W_{if}$, at the maximum value of σ_1'/σ_3', are 1.3 and
0.69 for the Garner and Bedford samples, respectively. A higher value of
$\delta W_{iD}/\delta W_{if}$ was correlated with the amount of rolling taking place within the

sample. In this case, the sample at a lower initial void ratio developed more rolling and it had a higher value of σ_1'/σ_3' than the sample at higher void ratio. This indicates that the Garner sample may be brought to a lower void ratio than the void ratio obtained with the sample preparation method used in this investigation. Therefore, the Bedford sample developed a relatively higher strength than the Garner sample with respect to their particular structure, even though the value of σ_1'/σ_3' was higher for the Garner than for the Bedford sample. This means that the "best" packing in terms of deformation and composition of the strength of the Garner sample was not achieved. "Best" packing is understood as giving a low value of the ratio $\delta W_{iD}/\delta W_{if}$ calculated at the maximum value of σ_1'/σ_3'.

Similar analyses may be performed with the Bedford and Garner samples tested at a confining pressure of 30 psi, as shown in Figs. 8, 12 and 13. The rate at which the function F is developed for samples at 30 psi is faster than the rate for samples at 80 psi. This indicates that the relative number of sliding contacts is higher for samples at 30 psi than for samples under a confining pressure of 80 psi. The higher pressures favored rolling rather than sliding. As a result values of the ratio $\delta W_{iD}/\delta W_{if}$ are lower for the samples at higher confining pressure.

Figure 14 shows the relation between maximum σ_1'/σ_3' and initial void ratio. Initial void ratio is the calculated void ratio after consolidation under the applied confining pressure has been completed. Maximum σ_1'/σ_3' decreases linearly as the initial void ratio increases for the Bedford sample. However, the slope of these lines decreases as consolidation pressure is increased, becoming parallel to the abscissa at a consolidation pressure of 80 psi.
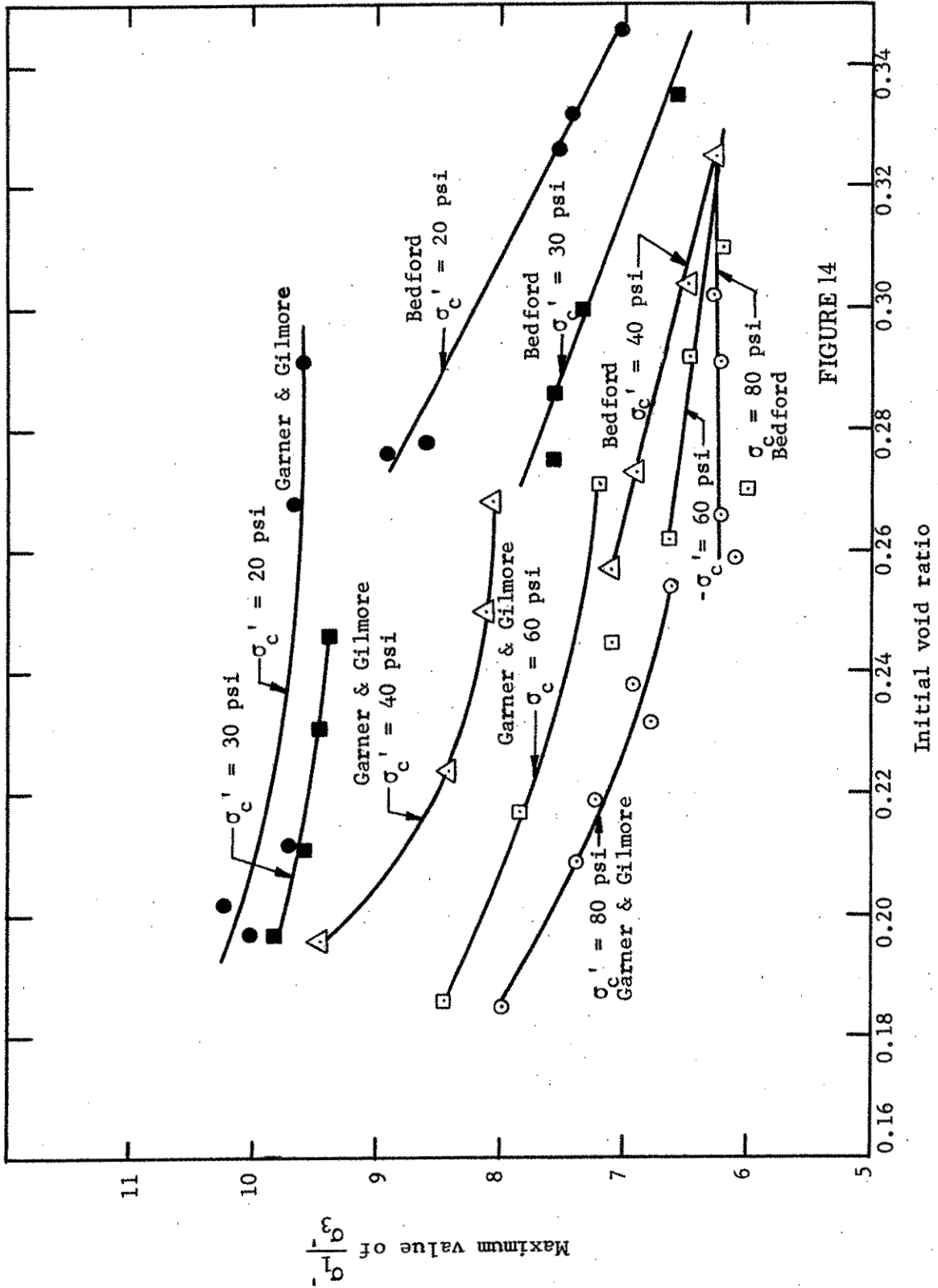
FIGURE 14

Maximum values of σ_1'/σ_3' versus initial void ratio were nearly

identical for the Garner and Gilmore samples and are so indicated on Fig. 14.

Maximum σ_1'/σ_3' decreases with increasing void ratio, although the slope of

each curve increases with increasing confining pressure. However, the curve

for 40 psi confining pressure indicated the greatest change in slope between

lower and higher initial void ratio, indicating that potential differences

between Gilmore and Garner stones may be reflected at this consolidation

pressure. Taylor[4] has shown that for uniform sand the maximum value of

σ_1'/σ_3' decreases in a linear fashion with increase in void ratio. However,

the slope of the lines is constant for different consolidation pressures even

though there is a parallel translation toward lower values of σ_1'/σ_3' as

the confining pressure is increased.

That the slope of relation between σ_1'/σ_3' and the initial void ratio

changes with increasing consolidation pressure and the values of ϑ decrease

with increasing consolidation pressure leads to the conclusion that the

deformation and strength of well-graded samples distinctively differ from

uniform or poorly graded samples*. The preceding also indicates that initial

void ratio cannot be used as a significant variable in the overall evaluation

of crushed limestones.

4. Summary

a. Theory presented by Tinoco and Handy[1] allows determination of

angle of solid friction, φ_s, whose value is solely dependent on the mineralogical

---

*If the octahedral stress is kept constant during the performance of a triaxial
test, the value of the parameter ϑ is reduced to zero, indicating that
interference between particles is reduced to a minimum. This also explains
why the maximum value of σ_1'/σ_3' is numerically higher at low confining
pressures than at higher confining pressures and explains the reduction of the
term $\delta W_{iD}/\delta W_{if}$ with increasing confining pressure.

composition of the particles. The average value of φ_s for the three crushed limestones used in this investigation is 34.2°.

b. The parameter $\mathcal{J}$ is a function of the gradation, particle arrangement, consolidation pressure and deformation history for the crushed limestones and allowed determination of the functions F, F', and D which describe the deformation behavior of the limestones.

c. Analysis of function F revealed that all samples underwent an initial compaction process, the extent of which, in terms of axial strain, depended upon the confining pressure. This initial compaction process, occuring during the early stages of deformation, influenced the amount of axial strain required to reach the maximum value of σ_1'/σ_3'. Initial compaction disappeared on reloading after the maximum value of σ_1'/σ_3' was reached. The modulus of deformation dependence on the confining pressure was explained to be due to this initial densification process.

d. Rate of change of function F with respect to the axial strain was related to the number and rate of formation of new sliding contacts.

e. Rate of change of functions F' and D with respect to axial strain was related to the number and the rate of formation of rolling contacts and depended upon the state of packing of the sample.

f. Effectiveness of packing of a given limestone sample, due to strength and deformational behavior, was related to the value of the ratio $\delta W_{iD}/\delta W_{if}$ calculated at the maximum value of σ_1'/σ_3'. Values of this ratio decreased with increased confining pressure and was further corroborated by the decrease in slope of the relation between the maximum value of σ_1'/σ_3' and initial void ratio as confining pressure was increased.

g. Maximum value of σ_1'/σ_3' should not be the single criterion on which crushed limestones could best be judged. Evaluation is best made by analyzing the relative effects of the various shear strength components.

h. Garner samples were found to give the best strength and deformational behavior, even though the "best" possible packing was not achieved with the sample preparation procedure used in this investigation. Gyratory compaction might prove more effective.

i. Bedford samples compacted to lower void ratios achieved the "best" possible packing but their overall behavior was rated below the other limestones. Changes in gradation of the Bedford sample could be made to improve its overall behavior. The exact nature of the necessary changes cannot be specified, although it may be recommended that:

(1) the percentage of material retained on a No. 10 sieve be reduced to levels between 50 and 60%;

(2) the percentage of sand size particles be increased in amounts corresponding to the reduction of the material retained on the No. 10 sieve.

j. Initial void ratio is not a significant variable in evaluation of strength and deformation characteristics of the crushed limestones.

B. Stability of Granular Mixes Compacted to Modified Density

This portion of the problem area evaluated the various factors, including shear strength, which influence the stability of crushed stone base course mixes compacted to modified Proctor density. All other portions of the study presented in this report deal with stability factors at standard Proctor compaction. Limited comparisons of the effect of both compaction efforts

are included in this portion of Problem Area 2. Reference is made to Best and Hoover[5] for a detailed analysis of this portion of the problem area.

1. Compaction

Modified Proctor density for each of the three crushed limestones was first determined in accordance with ASTM Designation D1557-58T, AASHO Designation T180-57, Method C. Following compaction, each specimen was weighed, extruded by hydraulic jack, and visually examined for segregation. After moisture content samples were removed, the remainder of each specimen was retained for mechanical analysis in order to determine the amount of degradation occurring during compaction. Results of the moisture-density relationships are shown in Fig. 15.

To determine the combination of factors necessary for vibratory compaction to modified Proctor density, with as little degradation and segregation as possible, the relationship between density and surcharge weight was investigated in a manner similar to that of Problem Area 1 for 4-in. diam by 9-in. high cylinders. A surcharge weight of 105 lb (8.35 psi), amplitude control dial setting of 90, and 2 minutes vibration time produced the most desirable results. No moisture-density relationships were determined for the vibratory compaction. However, initial moisture content greater than modified optimum was required for two of the materials; i.e., 1.1% moisture for Bedford, 0.3% for Garner and no additional for Gilmore. This increase may be due, in part, to the relative porosities of the materials. Little or no visible segregation was evident in the vibratory compacted specimens.

Several specimens were vibratory molded from each material to determine degradation. Average results of the mechanical analyses performed on specimens uncompacted, modified AASHO-ASTM, and modified vibratory compacted are given in Table 8. Due to the increased surcharge weight, slight degradation was
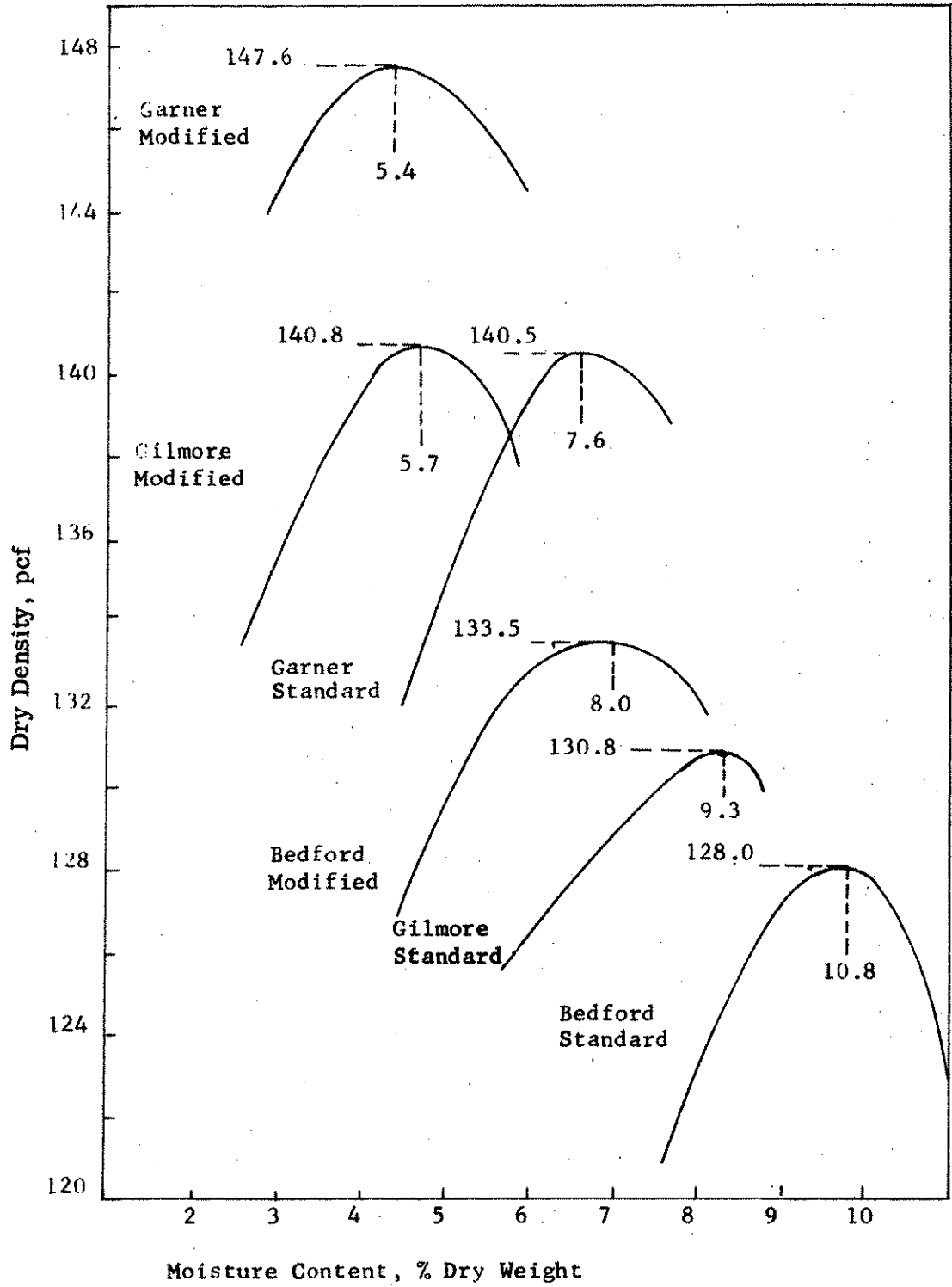
Figure 15. Moisture-density relationship of crushed stones

Table 8. Mechanical analysis of compacted crushed stone specimens.

Stone, type	Gravel[a]	Sand[b]	Percent of total Silt[c]	Clay[d]	Colloids[e]
Bedford					
Uncompacted	73.2	12.9	8.4	5.5	1.7
Modified AASHO-ASTM	65.8	15.0	11.8	7.4	1.9
Modified vibratory	68.8	14.6	10.2	6.4	2.0
Garner					
Uncompacted	61.6	26.0	10.2	2.2	1.4
Modified AASHO-ASTM	55.7	29.8	11.4	3.1	1.8
Modified vibratory	58.3	28.0	11.0	3.0	1.5
Gilmore					
Uncompacted	66.8	23.3	5.9	4.0	0.9
Modified AASHO-ASTM	62.0	26.2	7.4	4.6	1.6
Modified vibratory	64.3	24.8	6.9	4.0	1.4

[a] Particle size greater than 2.00 mm.

[b] Particle size 2.00 to 0.074 mm.

[c] Particle size 0.074 to 0.005 mm.

[d] Particle size less than 0.005 mm.

[e] Particle size less than 0.001 mm.

noticeable with modified vibratory compaction but was not as pronounced as with the modified AASHO-ASTM compaction process.

2. Shear Strength Criterion

Normal methods of interpretation of triaxial tests use a criterion of failure defined by consideration of stresses only. Such methods of investigation, when applied to granular base course materials, may result in only limited analyses of total stability.

The Mohr-Coulomb envelop enables a determination of the shear strength parameters φ and c. In addition, a modification of Mohr-Coulomb may be made and is termed the "stress path." Stress path is advantageous since each Mohr circle can be represented by a single point, the stress history can be visualized, the failure points of a number of specimens are exactly identified, and the shear parameters can be determined.

Of major importance in the use of Mohr-Coulomb or its modifications is the assignment of actual points of failure. Two common criteria for failure are maximum deviator stress, $\overline{\sigma}_1 - \overline{\sigma}_3$, and maximum effective stress ratio, $(\overline{\sigma}_1 - \overline{\sigma}_3)/\overline{\sigma}_3$. Some investigators advocate that when pore water pressures exist in soil specimens, maximum effective stress ratio is the true failure criterion, and at this point determine φ' and c'.

The mechanics of shear in a triaxial specimen of crushed stone must be considered for a better concept of failure. As the axial load is applied, a vertical deflection occurs. Since Poisson's ratio is generally believed to be greater than zero, the specimen tends to deform laterally and is resisted by the applied lateral pressure while compressing axially. This compression continues as the axial load is applied until some minimum volume is reached, the latter being a function of the applied lateral pressure and placement

density. During this loading, the pore pressure increases, causing a reduction in effective lateral and vertical pressures. When minimum volume is reached, the effective lateral pressure is not adequate to resist lateral deformation. For lateral deformation to occur, the particles must slide over one another. In granular soils this produces a significant volume increase as the particles rise up and over each other. This volume increase causes the pore pressure to reduce.

Some investigators have suggested that the point of maximum pore pressure and minimum effective lateral pressure coincide with the point of minimum volume and maximum stress ratio. However, in correlating the results of the study herein, it was observed that the point of maximum pore pressure coincided very closely with the minimum volume and both occurred at less percent axial strain than maximum effective stress ratio. The shear stress continued to increase as the volume increased until maximum effective stress ratio was reached. In addition, it was observed from stress path analyses that the limiting Mohr circle occurred at maximum effective stress ratio.

Thus, for the three crushed stones used in this investigation, the overall stability was best analyzed by observing the shear strength parameters, stress conditions, pore water pressure and strain characteristics at the point of maximum reduction of volume, i.e., minimum volume. Therefore, minimum volume becomes a condition of incipient failure, similar to "yield stress" in other materials.

3. Shear Strength Parameters

Table 9 presents the shear strength parameters for the three crushed stones. These results show that the angle of internal friction varied slightly from the failure criterion condition of minimum volume to that of

Table 9. Shear strength parameters for the crushed stones.

Material and compaction	Maximum effective stress ratio	Failure criterion	Minimum volume	
	φ' (degrees)	c' (psi)	φ' (degrees)	c' (psi)
Bedford-modified	43.6	13.46	44.8	1.28
Bedford + 200-modified	44.7	10.77	43.3	0.92
Bedford-standard	45.7	6.68	46.2	4.21
Garner-modified	48.6	18.30	48.6	3.73
Garner-standard	49.2	14.20	49.5	5.58
Gilmore-modified	46.8	18.07	46.6	8.75
Gilmore-standard	45.1	17.09	45.5	8.89

maximum effective stress ratio. The effect of particle interlocking[*] is reflected in the increased cohesion from minimum volume to maximum effective stress ratio. Change of compaction effort from standard to modified increased the amount of interlocking, and a higher cohesion value is shown at maximum effective stress ratio.

At minimum volume, increasing the density resulted in lower cohesion, again reflecting particle interlock. Specimens at standard density require more particle movement to reach minimum volume than specimens at modified density, and though expanded, this added energy results in higher values of cohesion.

In Table 9, the term "Bedford + 200 modified" refers to the Bedford crushed stone, all minus No. 200 sieve material removed, and modified compaction effort. Removal of the fines reduced both φ' and c' at minimum volume, which indicates a lowering of both frictional and cohesional strength due to an insufficiency of fines. In the whole Bedford sample, the quantity of fines may be overfilling the voids, increasing frictional and cohesive characteristics, and in turn indicating the need for determination of optimum percentages of minus No. 200 particles for particular granular materials compacted in place in a base course.

Variations in values of friction angle and cohesion may result from minor variances in void ratio, particle shape, size and porosity, gradation, surface texture, plasticity of the fines, and degree of saturation. Other

---

[*]Particle interlock is referred to as the increase in shear stress as the specimens expand from minimum volume to the point of maximum effective stress ratio and is the result of the work done by the specimen in increasing its volume during shear.

investigators have shown the dependence of friction and cohesion on the above
physical properties. Thus the use of the parameters φ' and c', as an overall
measure of the stability of granular base mixes, can be misleading.

4. Stress-Strain-Volume Change-Pore Pressure

Failure of base courses occurs when vertical deflection becomes
excessive or when there is lateral movement from under the loaded area.
These conditions can be represented by the percentage of axial strain and
volume change that occurs during triaxial testing with the minimum volume
conditions defining the failure point.

Figure 16 illustrates the strain-pore pressure-volume change versus
lateral pressure relationship, developed at the point of minimum volume, for
the Bedford stone. In general, the increase in density from standard to
modified improved the characteristics of the Bedford by lowering the strain,
pore pressure, and volume change values at each confining pressure. Similar,
though not as pronounced, results were obtained with the Gilmore and Garner
stones. It is also apparent in Fig. 16, as well as succeeding figures, that
the lateral pressure utilized in a base course has a direct effect on
stability.

Values of pore pressure of the Garner and Gilmore materials were signifi-
cantly less than the Bedford material and are probably of little consequence
in base course usage as long as capillary conditions are nonconducive to
moisture flow. For the Bedford sample, pore pressures ranged from near zero
to 10.0 psi with increasing lateral pressure. Stated differently, pore
pressure of the Bedford ranged up to near 1500 psf, adequately high to be of
considerable significance in the overall stability of base courses constructed
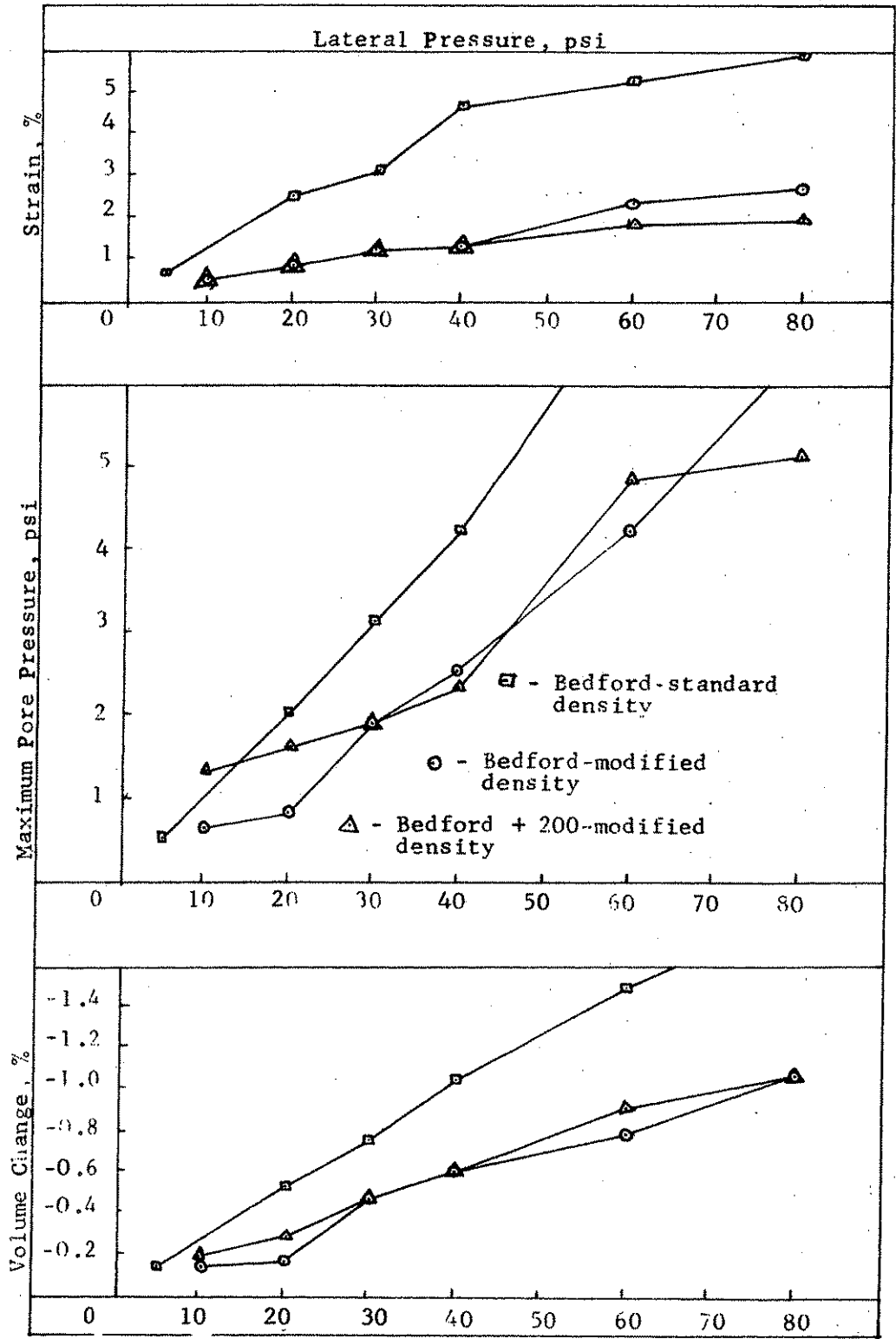
Figure 16   Strain-pore pressure-volume change versus lateral pressure
for Bedford stone

of similar materials. The necessity of preventing a high degree of saturation in a base course in obvious.

A factor which may reflect the pore pressure characteristics of a re-compacted crushed stone is the porosity of the whole stone. For example, the table below compares pore pressure measurements on the three materials for the two compaction conditions, at 80 psi lateral pressure, with porosity the same as that described on page 3 of this report.

Material	Compaction	Pore pressure at minimum volume (psi)	Porosity of whole stone (%)
Bedford	Standard	10.0	32
	Modified	7.2	
Gilmore	Standard	3.2	12
	Modified	1.4	
Garner	Standard	3.5	10
	Modified	3.6	

At standard density, both pore pressure and porosity of the Bedford sample are about three times those of Gilmore and Garner samples.

Figures 17 and 18 illustrate the general range of plots of deviator stress $(\bar{\sigma}_1 - \bar{\sigma}_3)$ versus axial strain of the three stones and are typical of granular materials ranging from "loose" to "dense", i.e., deviator stress increases to a maximum and then either remains constant or sharply decreases with increasing strain.

The strain required to produce maximum deviator stress appeared relatively independent of applied lateral pressure, but was dependent on type of stone,
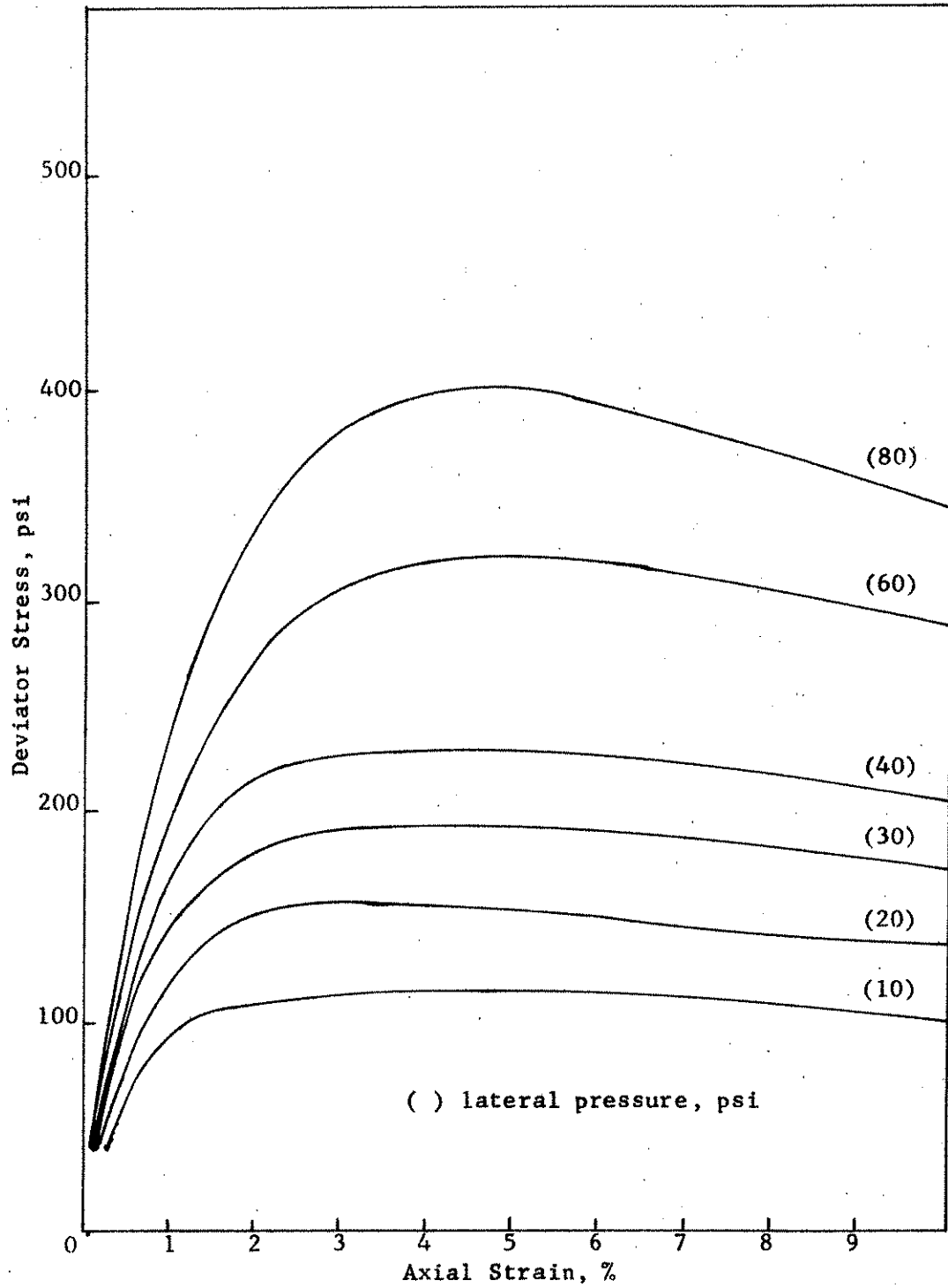
Figure 17. Deviator stress-axial strain curve for Bedford specimens
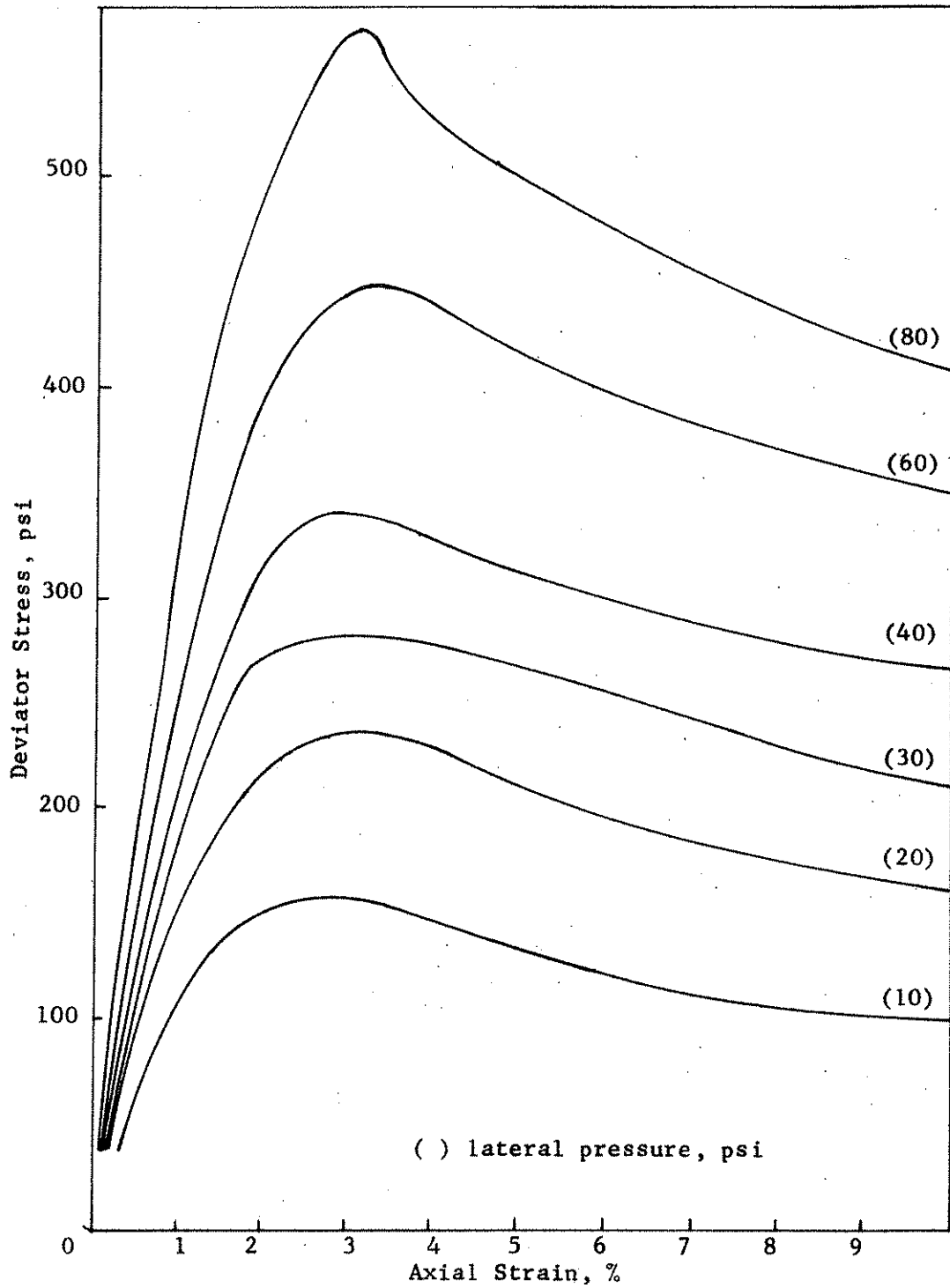
Figure 18. Deviator stress-axial strain curves for Garner specimens

being approximately 3% for the Garner and 5% for the Bedford and Bedford

+ 200. A large difference was indicated in the maximum deviator stress for

the stones at each lateral pressure; i.e., highest for the Garner and lowest

for the Bedford.

Only minor differences in maximum deviator stress were noted for

identical stones at the two densities. Figure 19 illustrates these differences

and is typical of all lateral pressures and stones. Increasing the density

resulted in an improvement in the stress-strain performance at low values of

strain, but beyond maximum deviator stress the stress-strain behavior was

about the same for both densities.

The relationship of stress to strain for soils does not always follow

mechanics of materials laws governing such relationships. For example,

there are several ways of defining a so-called "modulus of elasticity."

In this investigation a term "stress modulus" was defined as the deviator

stress $(\bar{\sigma}_1 - \bar{\sigma}_3)$ at minimum volume, divided by the corresponding strain,

and was used to relate the stress-strain characteristics at the failure

condition of minimum volume. Thus a plot of deviator stress versus strain at

minimum volume was produced, from which the value of "stress modulus" was

computed for each stone at each lateral pressure. Although the plotted

points were slightly scattered, Fig. 20 shows the trends of calculated

"stress modulus" versus lateral pressure for each material and density.

Two different behaviors are indicated: (a) the lateral pressure has no

effect on stress modulus, and (b) stress modulus increases with increasing

lateral pressure. The four materials of behavior (a) easily decrease to

minimum volume with an increase in stress and proportional amount of strain at
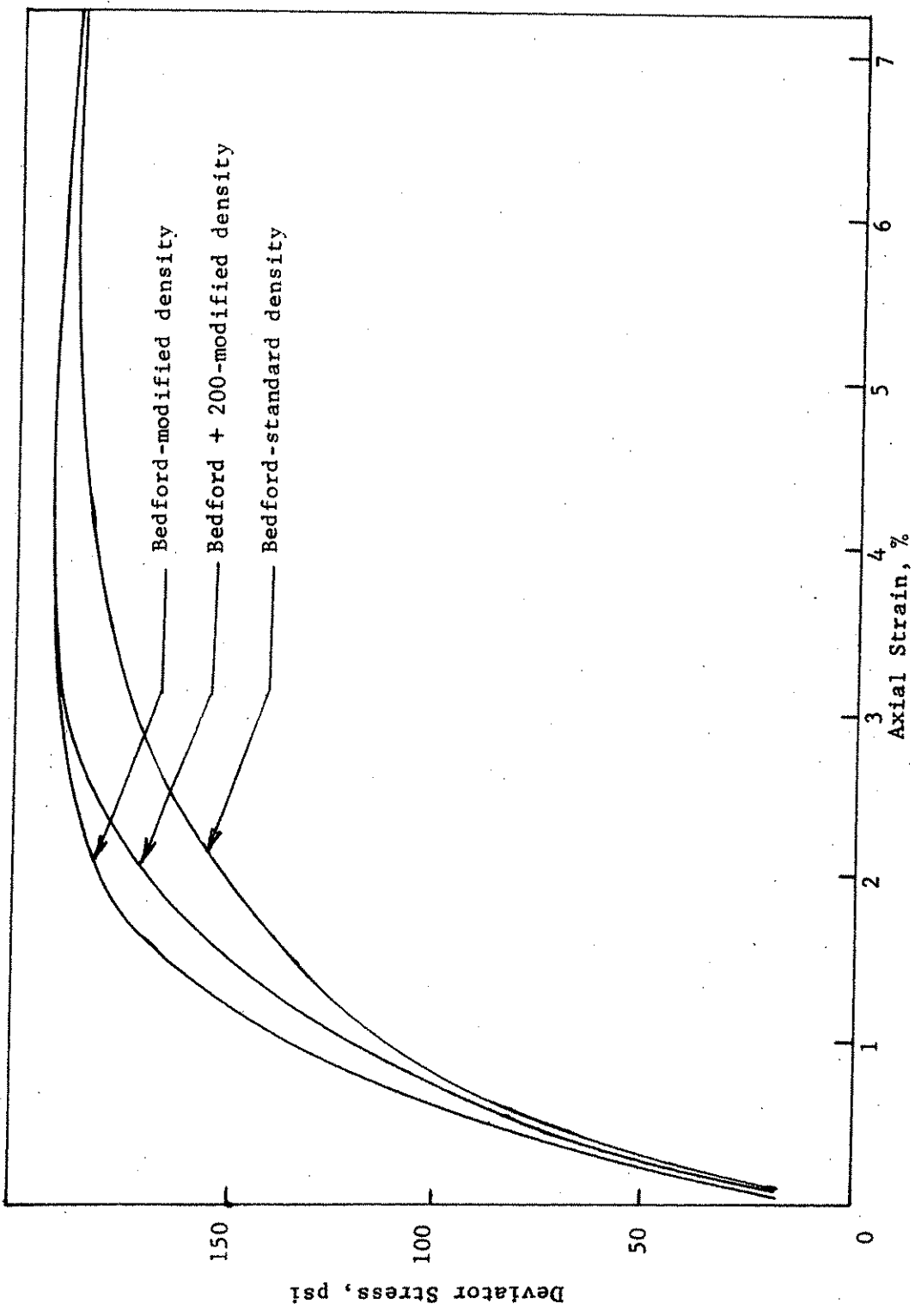
Figure 19. Deviator stress-axial strain curves for Bedford modified, Bedford + 200 modified, and Bedford standard at 30 psi lateral pressure
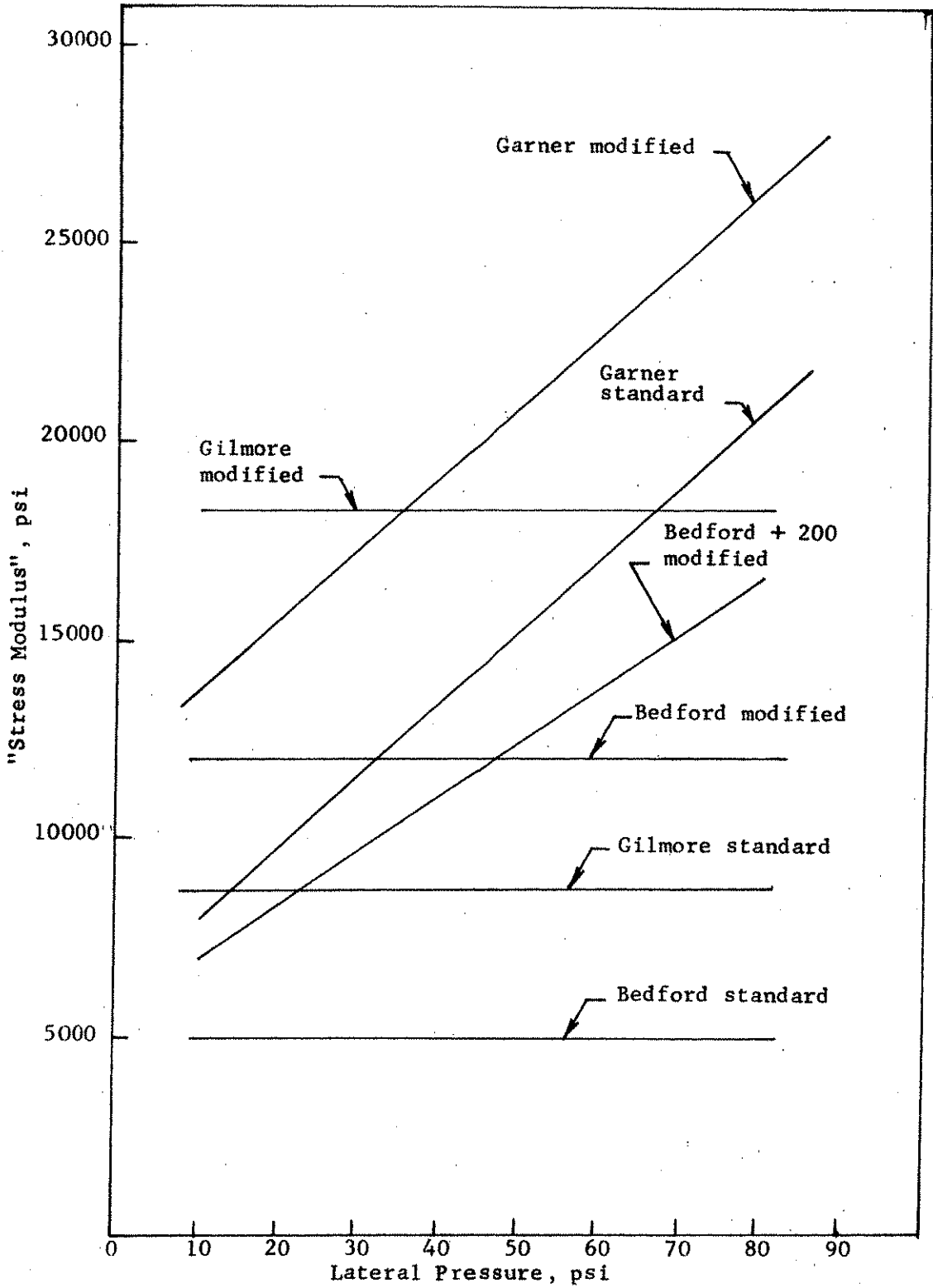
Figure 20. "Stress modulus" at minimum volume versus lateral pressure for the crushed stones

the different lateral pressures, and were the least dense of the stones investigated. The Garner stone, at a higher density, indicates that the stress to produce minimum volume is not proportional to the strain, as with the other materials, and its stress-strain stability is increased with increased confinement. Removal of the fines from the Bedford reduces any lubrication effect and is obviously not beneficial to the material at lower lateral pressures.

The stress modulus and lateral pressure relationship provides a reasonably good measure of the stones' stability. The steeper the slope or the higher the modulus value, the more stable is the material. This is verifiable to a degree because the Garner sample has the best field service record, while the Bedford sample has the poorest. However, the stress modulus concept also indicates that increases in density are beneficial since the values increased significantly between standard and modified compaction.

Figure 21 shows the deviator stress-volume change relationship for the modified density, Bedford + 200 specimen at 60 psi lateral pressure. It is typical of the above relationship for all the materials and also demonstrates the mechanism of failure discussed previously. As the deviator stress is increased, the specimen reduces in volume until reaching a minimum volume corresponding to the lateral deformation producing a volume increase. In these tests the lateral pressure was held constant resulting in a higher deviator stress beyond the point of minimum volume change. In field conditions, the lateral pressure may not remain constant, but may decrease when lateral deformation occurs. Therefore, the stress-volume change relationship may not exhibit an increase in stress as lateral deformation and expansion occurs, but would tend to decrease due to decreasing lateral pressure.
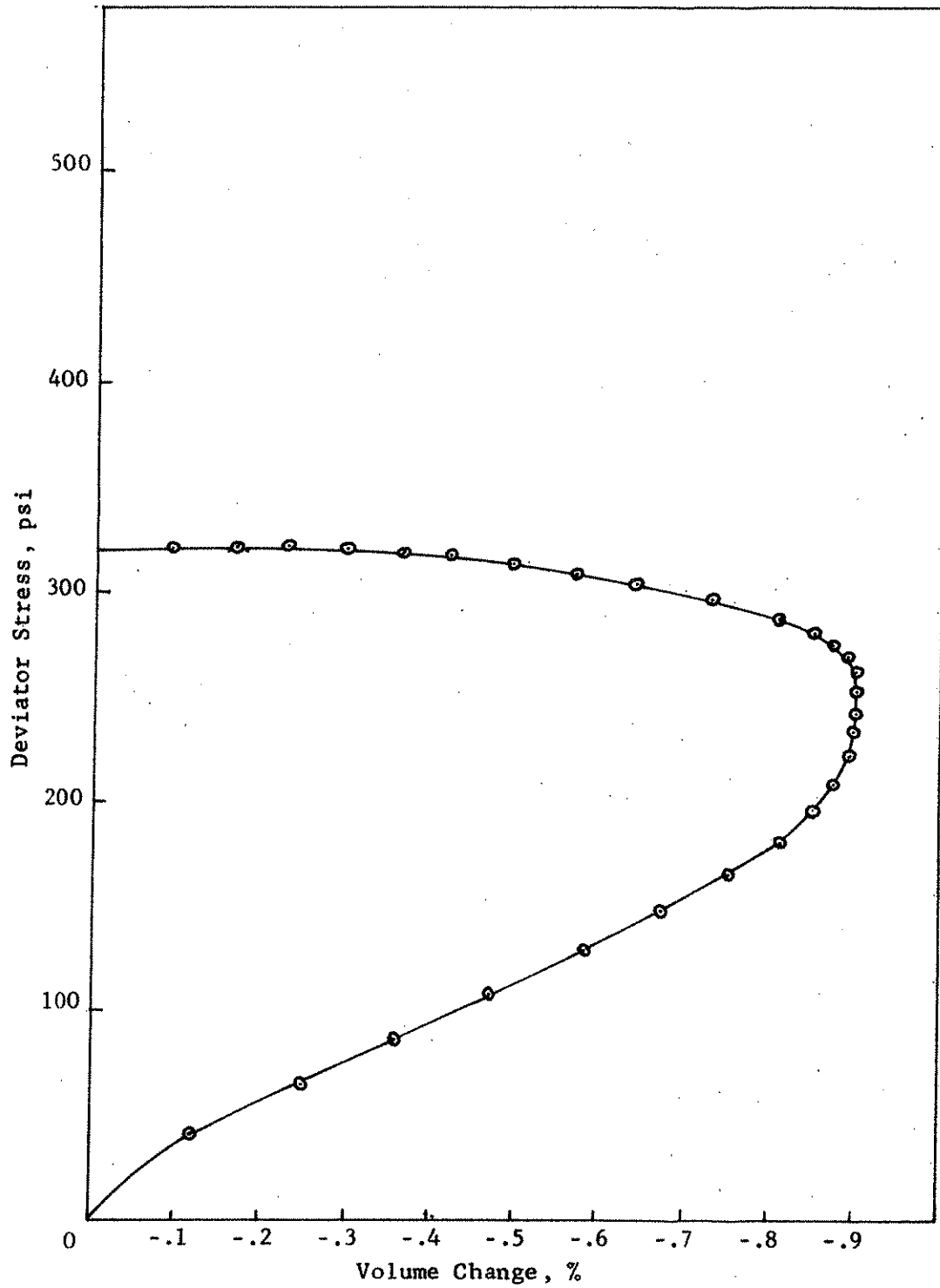
Figure 21. Deviator stress-volume change relationship for Bedford +
200 at 60 psi lateral pressure

Figure 22 relates the deviator stress and percent volume decrease at minimum volume and varying lateral pressure for all materials tested in this study. The steeper the slope of the deviator stress-volume change line, the more stable the material. The results indicate that the modified Garner, Garner standard, and modified Gilmore samples behave similarly in volume change characteristics. An increase in density improved the Bedford and Gilmore stones and produced a lower percentage of volume change under any given stress condition. Removal of the fines from the Bedford was detrimental since a lower stress was required to produce an equal percentage of volume change at minimum volume for the two Bedford materials at modified density.

5. Summary

a. Minimum volume condition appears to be a more valid failure criterion for granular base course mixes than maximum effective stress ratio or maximum deviator stress.

b. Use of only shear strength parameters may not be an entirely acceptable criterion for the determination of stability of granular materials.

c. Stability of granular materials should be evaluated in terms of the shear strength parameters, stress-strain, and stress-volume change relationships.

d. Stability of the crushed stones investigated appears to vary with the applied lateral pressure and initial state of densification.

e. Failure of granular base course materials may be controlled by the lateral pressure that can be developed within the base course regions.

f. Increase in density from standard to modified Proctor results in decreased strain, volume change, and pore pressures, improving the stability of the crushed stones. This increase in density has not significantly
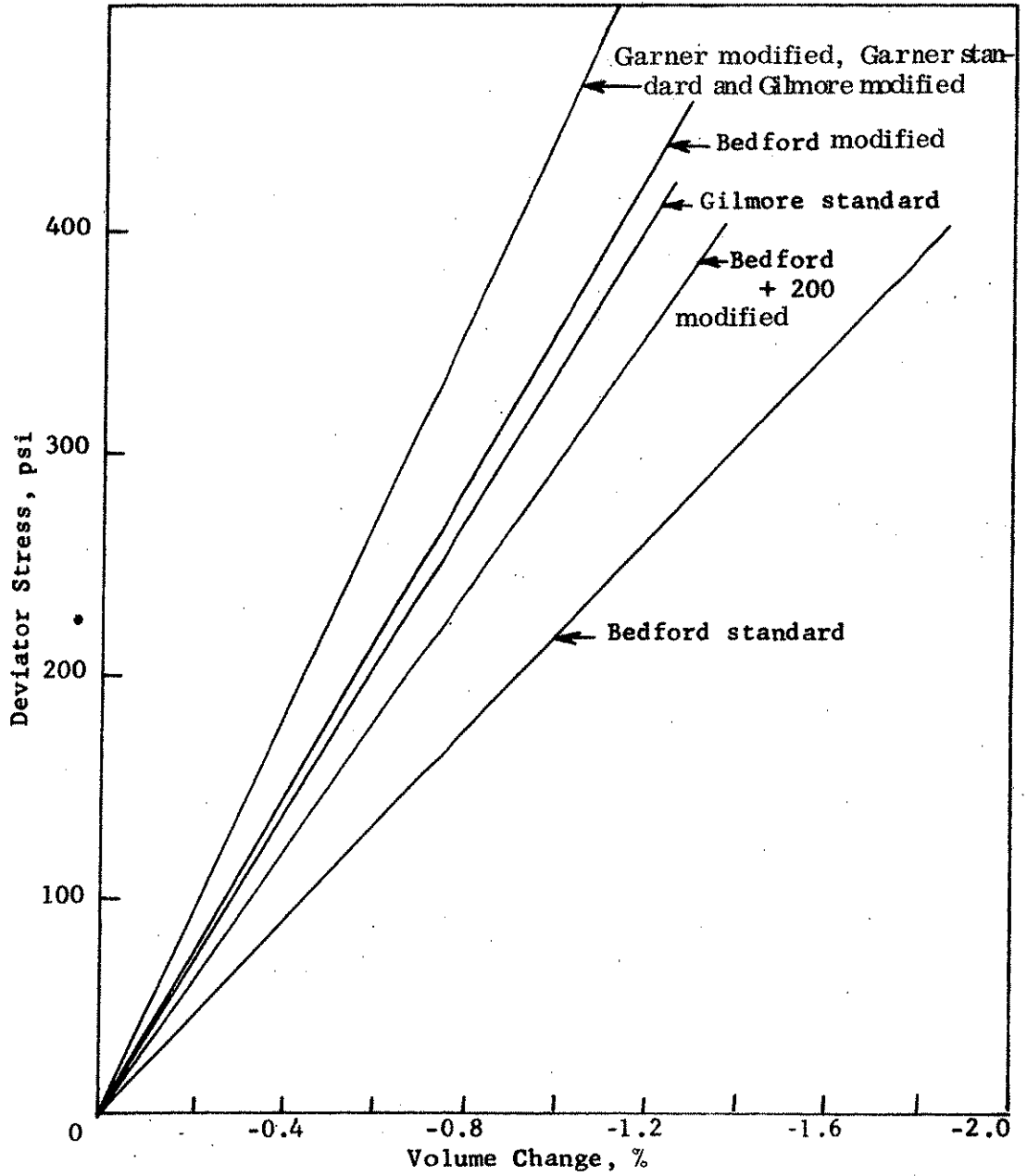
Figure 22. Envelopes of deviator stress-volume change at point of minimum volume for the crushed stones

changed the shear strength parameters or maximum stress that can be sustained by these stones.

g. Pore pressures become significant in granular materials that are at a high degree of saturation.

h. The Garner stone appears to have the greatest stability as measured by shear strength, stress-strain, and stress-volume change. Bedford stone appears to have the lowest stability as measured by the same relationships.

i. Removal of the minus No. 200 sieve portion of the Bedford stone did not significantly reduce its overall stability, but indicated that there may be an optimum percentage of materials passing the No. 200 sieve.

V. PROBLEM 3 — EFFECT OF STABILIZING AGENTS ON SHEARING STRENGTH

The purpose of this study was to investigate the effect of additions of various economically feasible stabilizing agents on the shear strength properties of the crushed stone materials. Knowledge gained in Problem Areas 1 and 2 assisted in this portion of the project, relative to methods of compaction, testing, and general stability analyses.

A. Treatment with Portland Cement

Two objectives were established for this portion of the study: (1) percentage of Type I Portland cement normally needed for maximum durability through freeze-thaw evaluation; and (2) effect of cement treatment on the overall stability of the crushed stones. Reference is made to selected bibiliography numbers 6 and 7 for detailed analyses of this portion of the problem area.

1. Durability Tests

Cement requirements for soil-cement mixtures are controlled by freeze-thaw tests (ASTM D560-57) and wet-dry tests (ASTM D559-57). Since soil-cement is primarily used in bases, rather than surface courses where wearing ability is an important criterion, the validity of a test where the samples are stiff-wire-brushed after each cycle of freeze-thaw could be questioned.

A laboratory freeze-thaw test for cement treated granular base materials that will more nearly duplicate field conditions (hereafter referred to as the Iowa Freeze-Thaw test) was compared to the ASTM D560-57 test. Also, a vibratory method of compaction was compared to the AASHO-ASTM standard compaction method for preparation of all freeze-thaw specimens[*]. Method B

---

[*]The AASHO-ASTM method of compaction is hereafter referred to as Method A, while the vibratory compaction is referred to as Method B.

was accomplished in much the same manner as vibratory compaction of the triaxial test specimens, except that a 4.00-in. diam by 4.585-in. high cylinder was produced. Specimen sizes in both methods of durability test were nearly identical.

Essentially, the Iowa freeze-thaw test consists of freezing the specimens from the top, with free water available at the bottom, and considers both strength and length change rather than brushing loss as criteria for design cement content.

Reproducibility of densities by the two compaction methods is indicated in Table 10. The series designation refers respectively to Bedford (B), Garner (G), and Gilmore (H), and cement contents (5,3 and 1%). Specimens compacted by Method A showed an overall average standard deviation in density of 1.25 pcf and a coefficient of variation 0.95%. Specimens compacted by Method B had an average standard deviation of 0.55 pcf and a coefficient variation of 0.40%. Vibratory compaction yielded more uniform densities than the standard drop-hammer process. The vibratory technique produced negligible amounts of degradation of particle sizes.

Portland Cement Association (PCA) recommends that soil-cement brushing losses for A-1, AASHO classified soils, be not greater than 14.0% by dry soil weight following 12 cycles of freeze-thaw. Studies by Packard and Chapman of the PCA have indicated that precise length change measurements are considered to be a very sensitive and **direct** measure of deterioration. Although no standard criteria of length change versus design cement content have been established, it was assumed in this study that cement requirements based on a minimization of length change might arbitrarily be made for comparative purposes only. Table 11 presents the results of the brushing loss

Table 10. Standard deviation and coefficient of variation of densities of specimens.

Series designation	Compaction Method A[a]		Compaction Method B[b]	
	Standard deviation (pcf)	Coefficient of variation (%)	Standard deviation (pcf)	Coefficient of variation (%)
B-5	0.93	0.73	1.14	0.89
B-3	0.61	0.49	0.39	0.31
B-1	1.28	1.03	0.38	0.30
Bedford ave.[c]	0.94	0.75	0.64	0.50
G-5	1.13	0.82	0.67	0.46
G-3	0.99	0.72	0.75	0.52
G-1	1.25	0.91	0.37	0.26
Garner ave.[c]	1.12	0.81	0.60	0.41
H-5	1.04	0.78	0.29	0.21
H-3	2.65	2.03	0.36	0.26
H-1	1.35	1.03	0.56	0.42
Gilmore ave.[c]	1.68	1.28	0.40	0.30
Overall average	1.25	0.95	0.55	0.40

[a]Each value computed from a series of 8 specimens.

[b]Each value computed from a series of 12 specimens.

[c]Each value is an average of the preceding 3 standard deviations or coefficients of variation.

Table 11. Relation of soil-cement brushing loss and length change to cement content.

Series designation	Compaction method A			Compaction method B		
	Length change (%)	Soil-cement loss (%)	Number F-T cycles	Length change (%)	Soil-cement loss (%)	Number F-T cycles
B-5	- 0.10	2.3	12	- 0.03	0.7	12
B-3	Failed	100	6	Failed	100	10
B-1	Failed	100	2	Failed	100	4
G-5	- 0.28	1.4	12	- 0.14	0.5	12
G-3	+ 0.34	11.3	12	- 0.14	1.4	12
G-1	Failed	100	3	Failed	100	6
H-5	+ 0.78	3.0	12	+ 0.06	0.4	12
H-3	Failed	100	5	Failed	13.2	12
H-1	Failed	100	1	Failed	100	5

and length change study.

In the Iowa freeze-thaw test the ratio of average unconfined compressive strength of freeze-thaw specimens at 10 cycles, P_f, to that of control specimens[*], P_c, is the index of resistance to freezing, R_f. Tentative criteria for durability suggests a minimum $P_f = 459 \pm 41$ psi, and $R_f = 80\%$. Suggested maximum length changes are 1.0% following the last freeze cycle or 0.5% following the last thaw cycle. Table 12 presents the results of the Iowa freeze-thaw test.

The standard freeze-thaw test often requires additional molding and testing of specimens to pinpoint design cement content since no convenient method of interpolation is apparent. For example, it was not possible to adequately graph soil-cement brushing losses versus percent cement and interpolate a design cement content, since end of test conditions were not equivalent. However, the Iowa test allows full plotting of P_f, R_f and length change versus percent cement for ease of interpolation of design cement content to the nearest 0.5% cement. This is possible since all specimens can be tested throughout the 10 freeze-thaw cycles.

Tables 13 and 14 present respectively a comparison of required cement contents from each test and the suggested content from length change data of the Iowa test. Of primary importance in Table 13 are the cement contents obtained by PCA brushing loss criteria, index of resistance, R_f, and compressive strength after freezing, P_f. In general, the Iowa test indicates a reduction in cement content ranging from 0.0 to 1.5%. Variation of

[*]During the test, identical specimens remain immersed in distilled water.

Table 12. Results of Iowa freeze-thaw test.

Series designation	Cement content (%)	Compaction method A[a]				Compaction method B[a]			
		P_c (psi)	P_f (psi)	R_f (%)	Length change following freezing (%)	P_c (psi)	P_f (psi)	R_f (%)	Length change following freezing (%)
B-5	5	757	770	95	0.0	969	951	98	0.0
B-3	3	338	170	50	3.4	317	281	69	2.6
B-1	1	134	41	31	5.7	227	109	48	7.4
G-5	5	1640	1595	97	0.0	2210	2010	91	0.2
G-3	3	845	815	96	- 0.4	1100	993	90	0.0
G-1	1	190	117	62	2.4	374	245	66	2.5
H-5	5	702	668	95	- 0.1	1315	1190	90	0.1
H-3	3	280	231	83	1.1	813	660	81	0.3
H-1	1	86	50	58	2.2	227	97	43	2.8

[a]Each value noted is the average of at least two specimen tests.

Table 13. Comparison of cement contents obtained with each durability criterion, freeze-thaw test procedure and compaction method.

Compaction method	ASTM freeze-thaw test					Iowa freeze-thaw test			
	Brushing loss		Length change			Index of resistance (R_f)		P_f	
	A	B	A	B		A	B	A	B
B-series	3.5-5	3.5-5	5	5		4.5	4	4.5	4
G-series	3	1.5-3	3-5	3		1.5	2	2	2
H-series	3.5-5	3	>5	5		3	3	4	2.5

Table 14. Suggested design cement contents based on interpolation of length change data in the Iowa freeze-thaw test.

Compaction method	Following thaw cycle		Following freeze cycle	
	A	B	A	B
B-series	5.0	4.5	4.5	4.0
G-series	1.0	2.0	2.0	2.0
H-series	4.5	2.0	3.5	2.0

compaction method is most pronounced in the brushing loss test and least in
the index to resistance criteria, indicating an element of validity of this
test method regardless of the method of lab compaction and potentially
of field compaction processes.

Following is a summation of the conclusions pertaining to the durability
study:

1. Relatively small additions of Type I Portland cement can increase
durability and compressive strength and decrease potential volume change upon
freezing of compacted crushed stone bases in Iowa.

2. The vibratory method of compaction yields more consistent laboratory
densities than does the ASTM compaction method. The vibratory process is less
time consuming and produces less degradation of particles during compaction.

3. The Iowa freeze-thaw test is easier to conduct and more nearly
duplicates actual field conditions of freezing and thawing than does the
ASTM test.

4. The Iowa freeze-thaw test allows considerations of strength and
length change as well as durability of cement treated granular base materials.

5. The Iowa freeze-thaw test facilitates obtaining a design cement
requirement by a simple plot of index of resistance to freezing, R_f, and
unconfined compressive strength after test, P_f, versus cement content. The
ASTM method often requires additional molding and testing of specimens to
pinpoint the design cement content since no convenient method of interpolation
is apparent.

6. Cement content by measurement of length change in the Iowa test,
appears to be more suitable (probably due to less actual handling of the
specimens) and more closely associated with other criteria in the test than

does length change measurements of ASTM specimens with the brushing loss test.

7. Accurate length measurements after the freeze cycle can be obtained in the Iowa freeze-thaw test, but due to recommended procedure, cannot be obtained in the ASTM freeze-thaw test.

8. Percentage of length change of Iowa test specimens is generally greater than that of ASTM specimens, and may be indicative of the severity of the test process through greater water attraction and adsorption during freezing.

9. Comparison of cement contents by PCA brushing loss and Iowa P_f indicated variations of 0.5 to 1.0% cement. Comparison of brushing loss and R_f indicated variations of 0.5 to 2.0% cement. In each comparison, Iowa criteria indicated less cement content was required.

10. Vibratory compaction usually resulted in slightly lower design cement contents than did the ASTM compaction method.

2. Effect of Cement Treatment on Stability

Type I Portland cement contents were set at 0, 1 and 3% by dry weight, generally less than acceptable for freeze-thaw durability criteria. Field tests have shown that cement-modified crushed limestones perform satisfactorily, resulting in a general improvement of the frictional properties from that of the untreated material. Curing periods of specimens were both 7 and 28 days.

Analyses of this portion of the study generally followed the criteria set forth in section B of Problem 2; i.e., the overall stability was analyzed by observing the shear parameters, stress conditions, strain and pore water pressure characteristics, at minimum volume. Results are also reported for the failure condition at maximum effective stress ratio to further indicate

justification for minimum volume criteria as a condition of failure.

Table 15 shows that the magnitude of difference in values of cohesion, c', and angle of internal friction, ϕ', at the two conditions of failure may be an indication of the amount of interlocking within the granular materials. Shear strength based on the failure criterion of maximum effective stress ratio is normally greater due to the interlocking of particles, and generally results in increased cohesion coupled with a slight decrease in friction angle. All untreated materials in this investigation analyzed by the two criteria of failure followed the above pattern. The addition of cement in the Bedford and Gilmore stones resulted in similar shifting of shear parameters when analyzed by the two failure criteria but were of greater magnitude than those of the untreated.

Previous investigations have shown that cement treatment of granular materials results in a relatively constant angle of friction, whereas cohesion increases rapidly with increased cement content. Addition of increasing amounts of cement to the three crushed stones in this investigation produced varying values of the shear strength parameters. Cohesion of the treated Bedford stone increased by as much as 72 psi, while the angle of friction remained relatively constant, as compared with the untreated specimens. Cohesion of the treated Garner stone increased nearly linearly with increase in cement content after 28 days cure; however, ϕ' reduced slightly at 1% cement then increased at 3% cement content. Addition of 1% cement to the Gilmore stone produced relatively no change in cohesion but increased ϕ' by about six degrees above that of the untreated. At 28 days cure, the addition of 3% cement in the Gilmore sample produced no additional change in ϕ' but significantly increased cohesion. Addition of 1% cement in the

Table 15. Shear strength parameters.

Material and treatment	Maximum effective stress ratio		Minimum volume	
	ϕ' (degrees)	c' (psi)	ϕ' (degrees)	c' (psi)
Bedford crushed stone:				
Untreated	45.7	6.7	46.2	4.2
1% cement 7-day cure	47.0	24.2	47.9	15.9
1% cement 28-day cure	44.6	42.5	45.5	29.6
3% cement 7-day cure	47.0	67.0	47.7	56.6
3% cement 28-day cure	45.3	78.7	46.0	70.5
Garner crushed stone:				
Untreated	49.2	14.2	49.5	5.6
1% cement 7-day cure	54.6	21.6	53.1	9.2
1% cement 28-day cure	49.0	41.2	46.3	30.4
3% cement 7-day cure	50.1	90.5	50.6	64.6
3% cement 28-day cure	51.0	96.2	51.2	87.9
Gilmore crushed stone:				
Untreated	45.1	17.1	45.5	8.9
1% cement 7-day cure	50.6	18.1	51.8	0.8
1% cement 28-day cure	51.2	18.2	51.5	3.2
3% cement 7-day cure	48.6	57.4	49.0	43.8
3% cement 28-day cure	50.6	64.0	51.1	52.3

Failure criteria

Gilmore sample may not result in a complete cementation, or bonding of the large aggregate, but rather in a bonding of the fines, increasing the interlocking frictional effects between the stabilized fines and the larger aggregates.

Addition of cement to the three crushed stones reduced pore pressures to insignificant quantities. Change of pore pressure from failure conditions of minimum volume to maximum effective stress ratio indicated the magnitude of expansion during this phase of shear.

Cement treatment reduced the quantity of strain required to achieve ultimate strength by either criteria of failure when compared with the untreated materials. Magnitude of strain at failure for all three treated stones was relatively independent of lateral, or confining pressures, but appeared to vary with cement content and length of cure, i.e., decreased with increasing cement content and cure period. Magnitude of strain at failure of the untreated stones generally increased with increasing lateral pressures.

Analysis of volume change characteristics of the cement treated materials led to the premise that shear strength analysis alone does not fully explain the behavior of a granular material under actual field conditions. As untreated materials were axially loaded, there occurred a reduction in volume as well as a small quantity of lateral strain. In a base course, tendency for lateral expansion may be resisted by the adjacent material resulting in increased lateral support. This suggests that stability of a granular material is not entirely a function of the shear strength but must also be a function of the lateral restraining support that can be developed and the amount of expansion required to achieve this support.

The preceding form of stability may be illustrated by Fig. 23. Assume that a low lateral pressure exists in a base course material prior to the application of an axial load. As the load is applied, the base will deflect vertically downward until a point of minimum volume is achieved after which horizontal expansion increases rapidly, resulting in increased lateral support and increased bearing capacity. This progressive increase in lateral support will continue until a limiting value of lateral support is achieved, indicating that the stability of a granular material is not entirely a function of the shear strength. It must also be a function of the lateral support that can be developed and of the expansion required to develop that lateral support.

To visualize Fig. 23, assume an imaginary line tangential to the curves of Fig. 23, beginning at zero volume change and moving up to the left towards 700 psi effective stress. The points of minimum volume for each lateral pressure condition are close to this line. As the axial load is applied, at a low lateral pressure, the stress increases to the point of minimum volume, lateral expansion starts, confining pressure increases, and the process is repeated until a limiting value of confinement (dependent on restraint of shoulder, surcharge, and type of material) is achieved.

The mode of failure in a base course is probably due to progressive buildup of lateral support by lateral expansion of the loaded material. Prior to lateral expansion, the strength properties may be those of the laboratory tested material, but after lateral expansion occurs the strength properties of a given core of material are dependent upon the surrounding material.

Initial compression under a small increment of strain has been referred to

as elastic compression because the elastic Poisson's ratio is less than

0.5. As strain increases, expansion predominates because the elastic Poisson's

ratio may be greater than 0.5. Reaction of the Bedford specimens, with respect

to volume change and axial strain, is illustrated in Figs. 24 and 25 (Gilmore

and Garner materials followed very similar patterns). Initial slope of the

curves represent a degree of magnitude of Poisson's ratio. Since Poisson's

ratio is the ratio of lateral to vertical strain under axial loads, it can

be shown that when strain equals zero, volume change is equal to axial strain

and the material is in a compressed state. Likewise, for a noncompressive

material and a Poisson's ratio of about 0.5, both lateral and vertical strains

are finite quantities and rate of volume change is near zero.

As shown in Figs. 24 and 25, cement treatment of the Bedford material

shifts the axial strain-volume change curves closer to the condition of zero

lateral strain than with the untreated. The failure point of minimum volume

is also much closer to this line for cement treatments. Thus, the amounts of

both lateral and vertical strains developed in a treated specimen during

axial loading may generally be reduced, as compared to the untreated materials,

up to the point of failure.

Slope of the volume-change-strain curves of the untreated materials is

closer to the condition of Poisson's ratio equal to 0.5, indicating the

material is undergoing a limited amount of lateral strain even though volume

is decreasing. Slope of the volume change-strain curves for the cement

treated materials is closer to the condition of Poisson's ratio equal to

zero, which occurs only when lateral strain is small. Using the previous

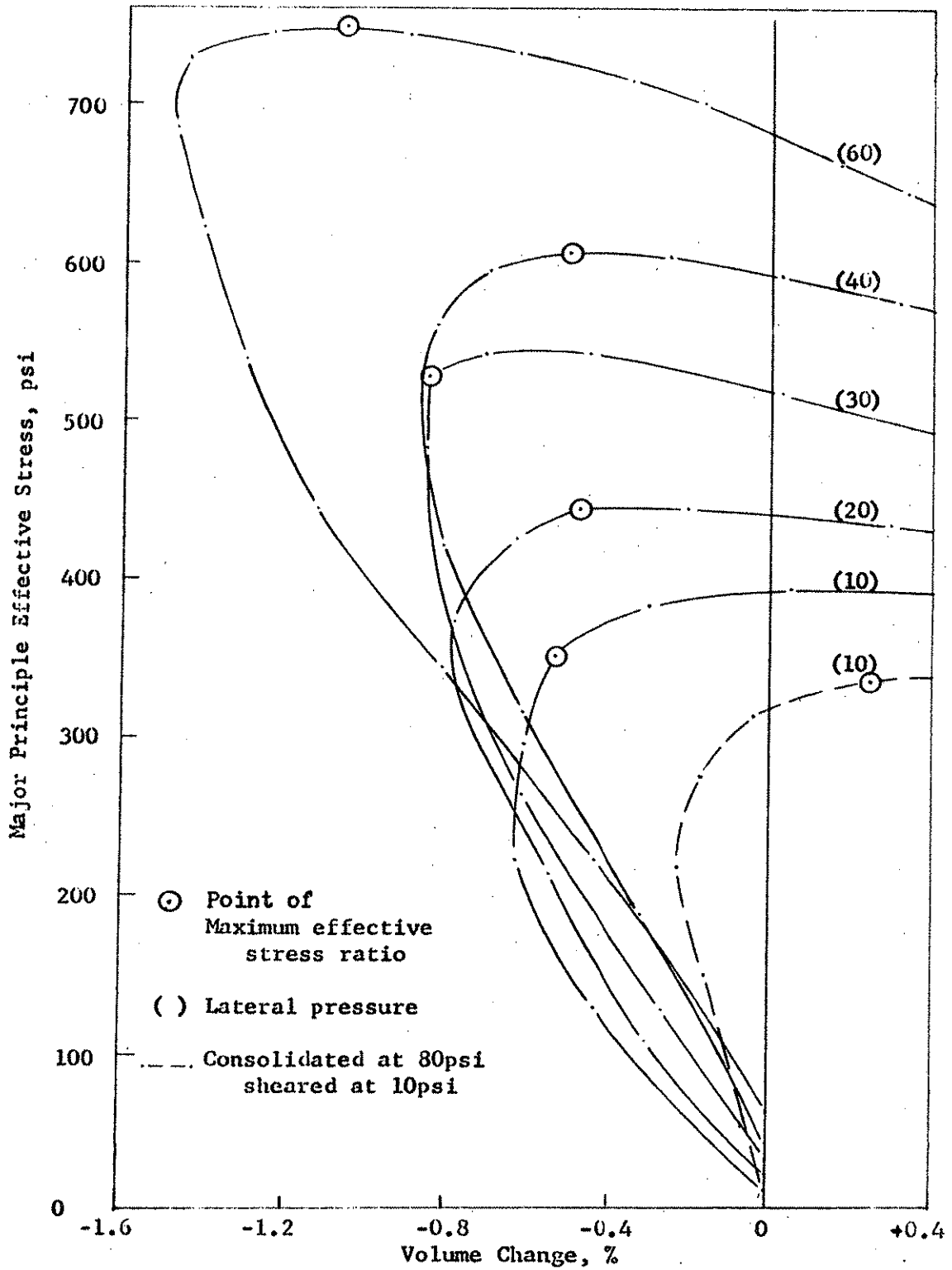assumption that lateral strain increases lateral support, the cement treated

Figure. 23. Major principle effective stress versus volume change for Bedford, 3% cement treatment, 7-day cure
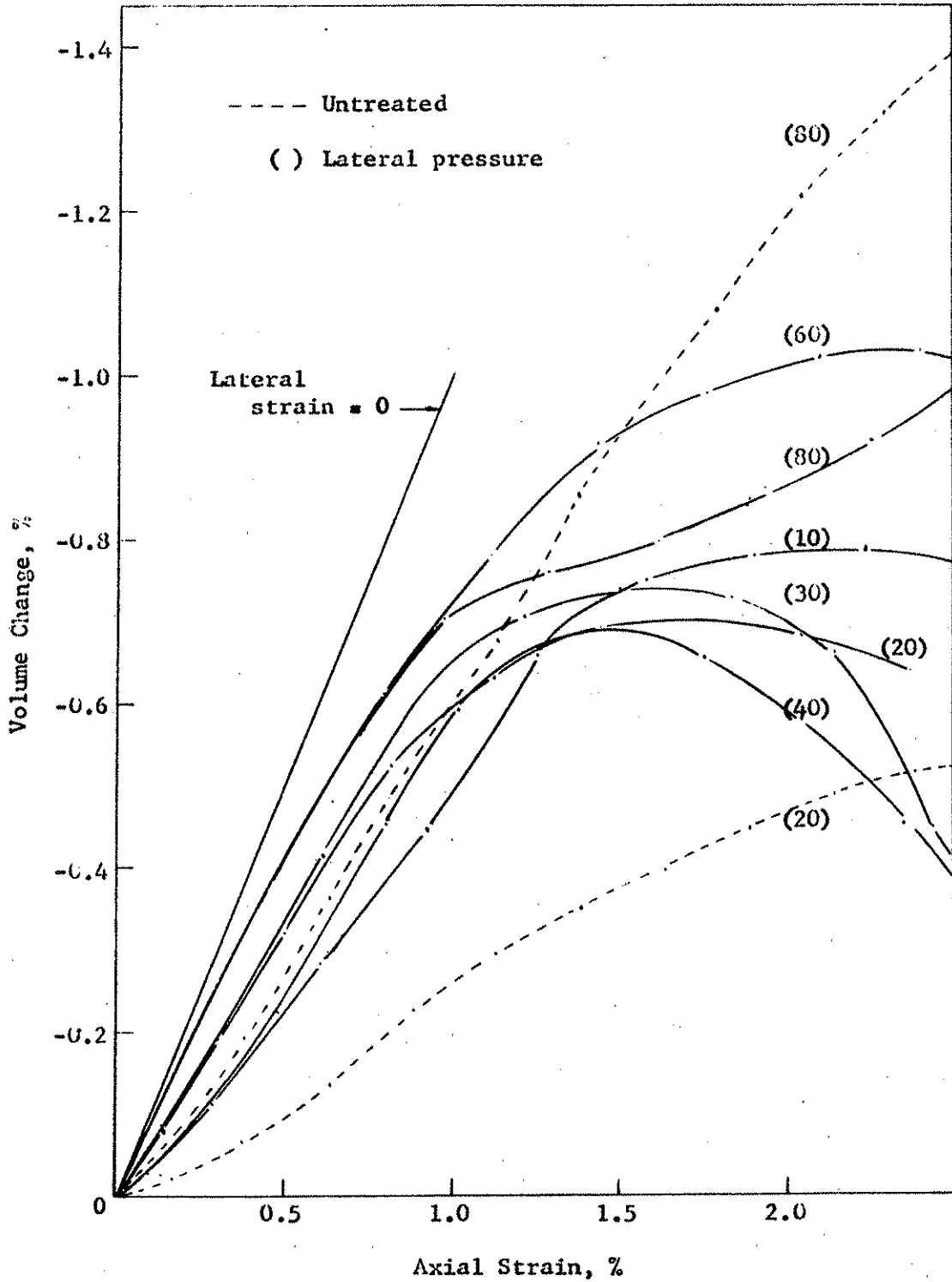
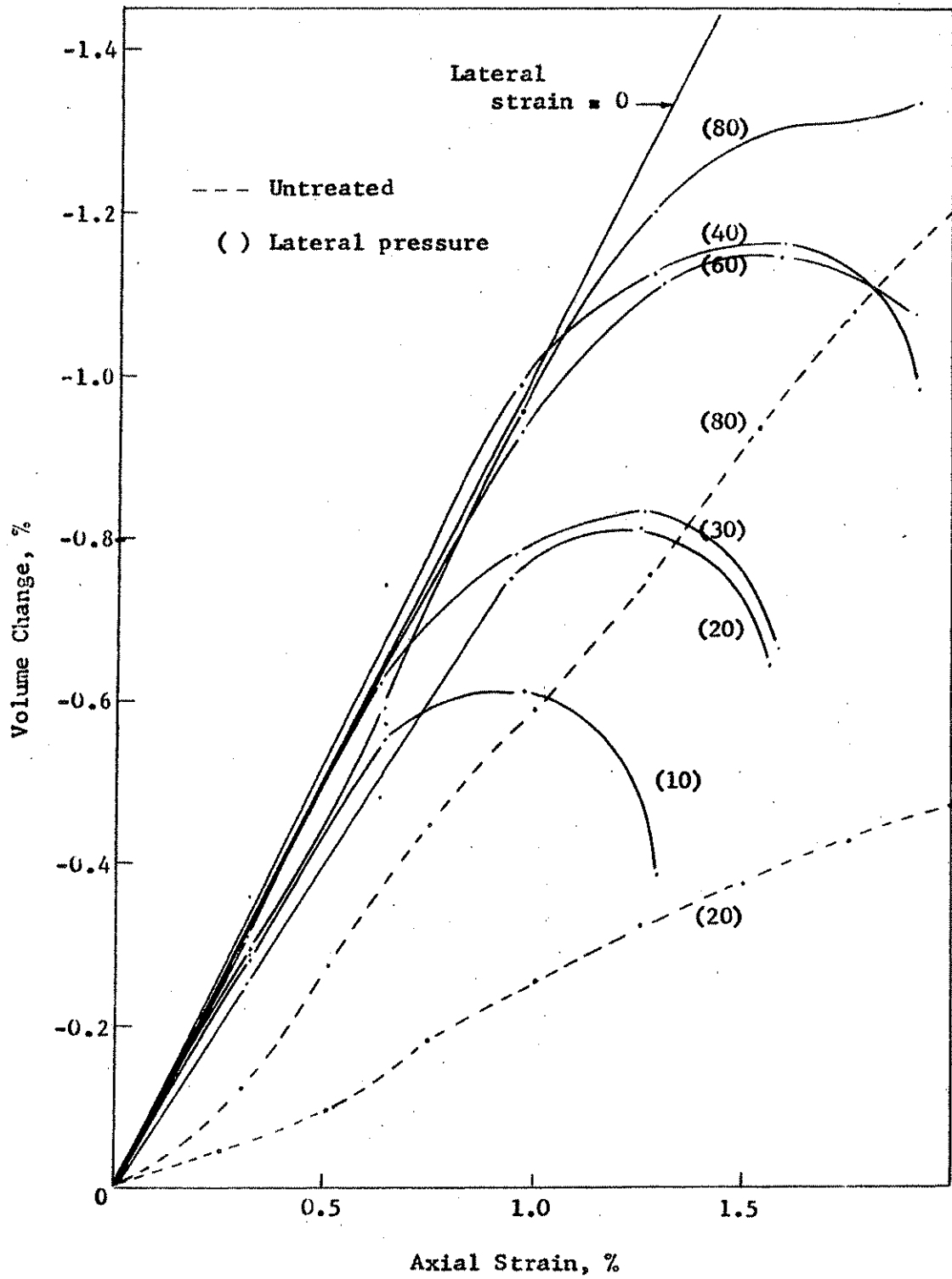Figure 24. Volume change-axial strain relationship for Bedford, 1% cement treatment, 7-day cure

Figure 25. Volume change-axial strain relationship for Bedford, 3% cement treatment, 7-day cure

materials have little tendency to increase lateral support prior to the
point of mininum volume due to the small amount of lateral strain developed.
Effective stresses at the point of minimum volume, as determined in a laboratory
test, should therefore be closely related to shear strength occurring under
field conditions.

Shrinkage cracking could be detrimental to the strength of a cement
treated base due to a reduction of lateral support in the region of any
cracking. If the amount of shrinkage is excessive, a large amount of lateral
deflection would be required to build up lateral support which can only occur
after the ultimate strength of the material is exceeded and the bonds begin
to rupture. This process could occur adjacent to cracks in the base course
and, although it might increase the amount of lateral support, the overall
stability might actually be reduced. The smaller the quantity of cement added,
however, the less the magnitude of cracking of cement treated crushed stone
bases. While shrinkage studies were not conducted as a part of this research,
it is generally thought that up to 3% cement by dry weight would not result
in excessive cracking, while maintaining a much higher degree of total stability
than the untreated stone.

B. Treatment with Bituminous Additives

Reference is made to the work of Whisler and Hoover[8] for a detailed
analysis of this portion of the problem area.

Two asphalt constituents, SS-1 slow setting emulsified asphalt and an
asphalt cement of 120-150 penetration, were selected for bituminous stabilization
of the three crushed limestones. Treatment levels with the two constituents

were 3% residual asphalt by dry aggregate weight for the emulsion and 4%

for the asphalt cement. Triaxial tests of the emulsion treated specimens

were conducted at room temperature while the asphalt cement specimens were

triaxially tested at 100°F.

The major failure criterion utilized was that of maximum deviation

stress, $\bar{\sigma}_1 - \bar{\sigma}_3$, or maximum effective stress ratio, $(\bar{\sigma}_1 - \bar{\sigma}_3)/\bar{\sigma}_3$, since:

(a) either criteria produced very similar results; (b) at either criteria, all

stability factors appeared to have the greatest numerical value; and (c) in

contrast to previous portions of Problem Area 3, minimum volume occurred at

a greater strain than represented by either maximum deviator stress or

stress ratio. This latter point is discussed in a succeeding section.

Three methods were used to determine the shear strength parameters of

each mixture; i.e., the Mohr envelope, a stress path approach, and a method

of least squares used by the Bureau of Reclamation, based on the Mohr envelope

concept. Table 16 presents φ' and c' results of the treated and untreated

materials. The values show little variation of angle of friction and

cohesion for the individual mixes analyzed by each method, and thus verify a

straight line envelope of failure.

Generally, asphalt treatment of the stones lowered the effective angle

of internal friction and increased the effective cohesion, although lowering

of the one parameter was roughly offset by the increase in the other.

Reduction of φ' is attributed to lubrication and separation of particles

by the asphalt film, while increase in cohesion is derived from the binding

characteristic of the film. Removal of all fines from the AC treated

Bedford sample indicated little effect on the shear parameters. Thus, it

Table 16. Shear strength parameters for bituminous treated and untreated crushed stones.

Material and treatment	Mohr envelope		Stress path		Bureau of Reclamation	
	φ' (degrees)	c' (psi)	φ' (degrees)	c' (psi)	φ' (degrees)	c' (psi)
Bedford:						
untreated	46.2	7.0	45.5	6.6	45.7	6.7
SS-1 emulsion (3.0% asphalt)	39.5	15.5	39.6	15.8	38.6	16.0
4.0% asphalt cement	41.2	10.5	41.6	10.7	41.0	11.8
4.0% asphalt cement (Sample less -200 material)	38.9	17.0	39.0	15.4	38.9	17.0
Gilmore:						
untreated	46.6	12.0	46.2	13.4	46.2	13.2
SS-1 emulsion (3.0% asphalt)	41.6	17.9	40.6	19.4	41.6	17.9
4.0% asphalt cement	42.4	14.4	42.4	14.4	42.3	15.8
Garner:						
untreated	50.2	11.0	49.8	13.9	49.3	14.2
SS-1 emulsion (3.0% asphalt)	45.3	18.7	45.5	16.9	45.5	17.3
4.0% asphalt	42.9	16.8	42.9	16.0	43.7	15.9

was impossible to determine complete success or failure of the asphaltic treatments based solely on φ' and c'.

Comparison of volume change, pore water pressure, and axial strain at maximum deviator stress more significantly shows the affects of asphaltic treatment of crushed stones. Figures 26, 27 and 28 present the above comparisons for the AC treated materials. Similar relationships were noted with the emulsion treatment. A composite comparison is as follows:

1. Maximum deviator stress of the untreated and treated stones increased with increasing lateral pressures. At low confinement, maximum deviator stress of the treated stones was equal to or slightly greater than the untreated. As confining pressures increased, corresponding increases in maximum deviator stress of the untreated materials were greater than the treated.

2. Percent volume change versus lateral pressure indicated only slight improvement due to treatment with asphalt at low confinement pressures. As lateral pressures were increased, percent volume change for all mixes decreased from positive or near zero values to negative values, i.e., from volume increase to volume decrease at failure. Volume change improvement was not noticeable at low lateral pressures with the Bedford AC treatment. Volume change of the untreated and emulsion treated Bedford were nearly identical.

3. Due to the porosity of the Bedford stone, the particles were not as effectively covered by the asphalt additives as were the Garner and Gilmore particles. However, bituminous treatment of the Bedford sample notably improved the pore pressure values apparently by waterproofing and sealing the pores of the stone, at least during the test. Waterproofing reduced excessive high and low pore pressures of the untreated Bedford stone at corresponding
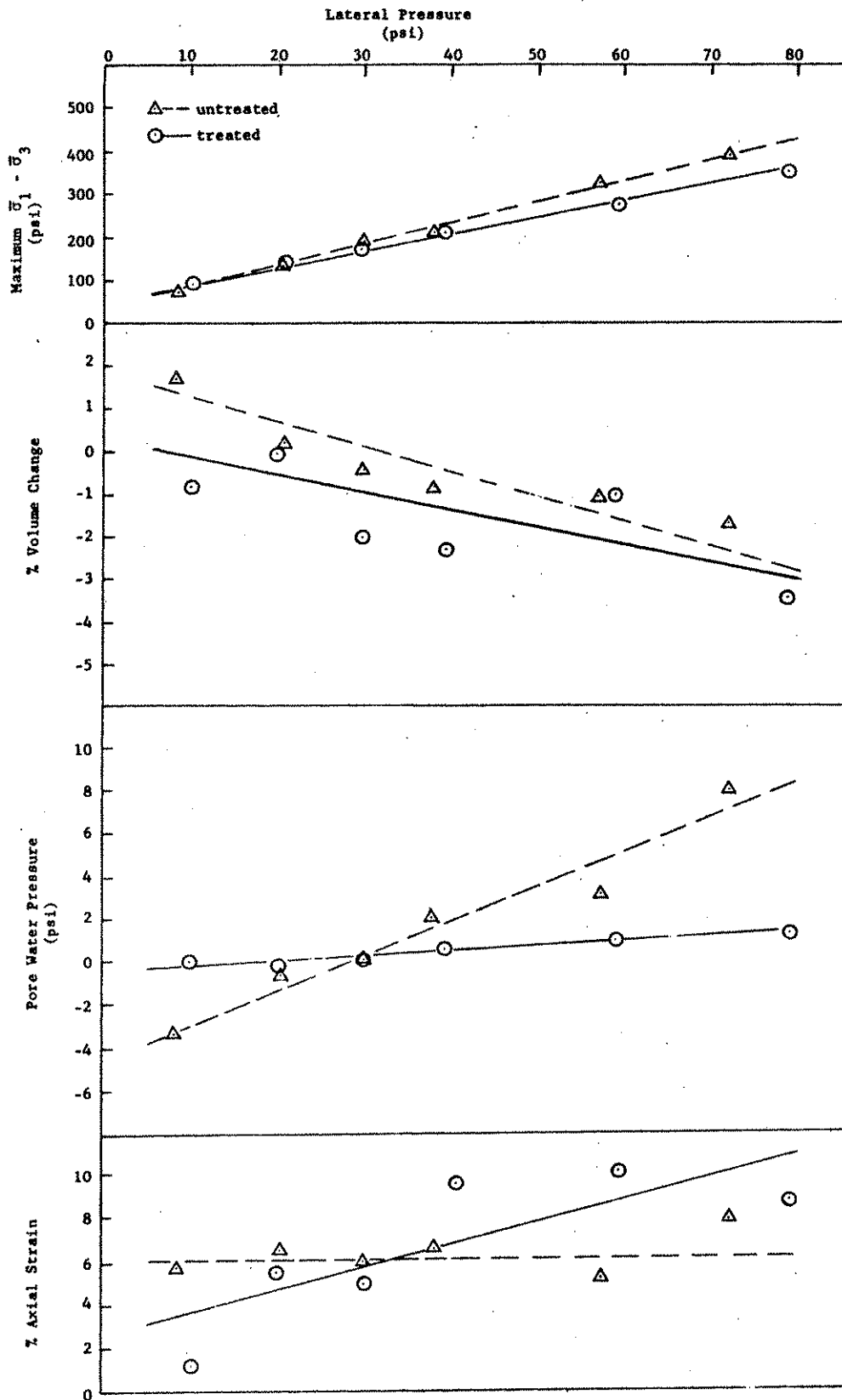
Figure 26. Percent volume change, pore water pressure, and percent axial
strain, at maximum deviator stress for untreated and asphalt
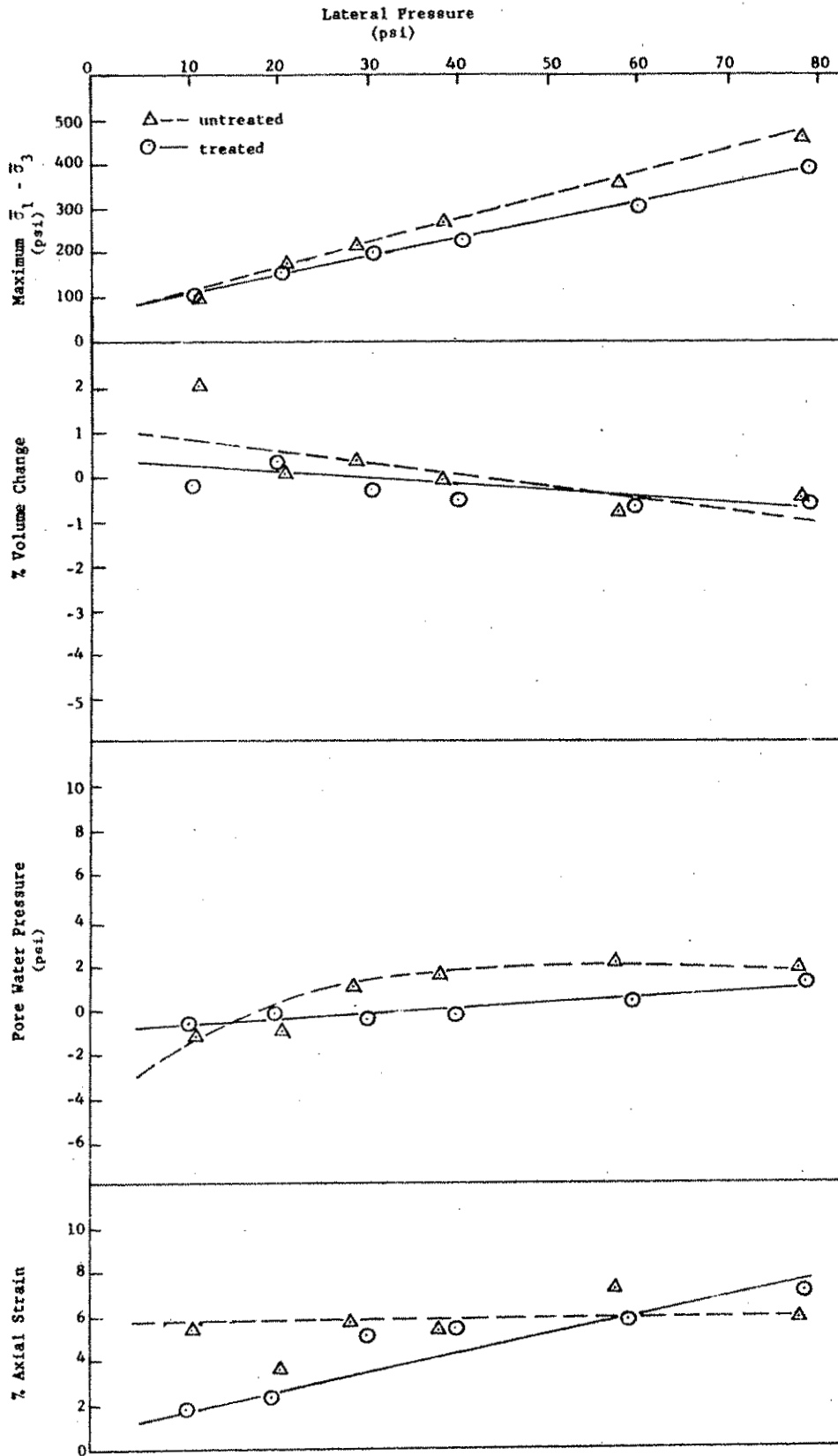cement treated Bedford specimens tested at varying lateral pres-
sures

Figure 27. Percent volume change, pore water pressure, and percent axial strain, at maximum deviator stress for untreated and asphalt cement treated Gilmore specimens tested at varying lateral pressures.
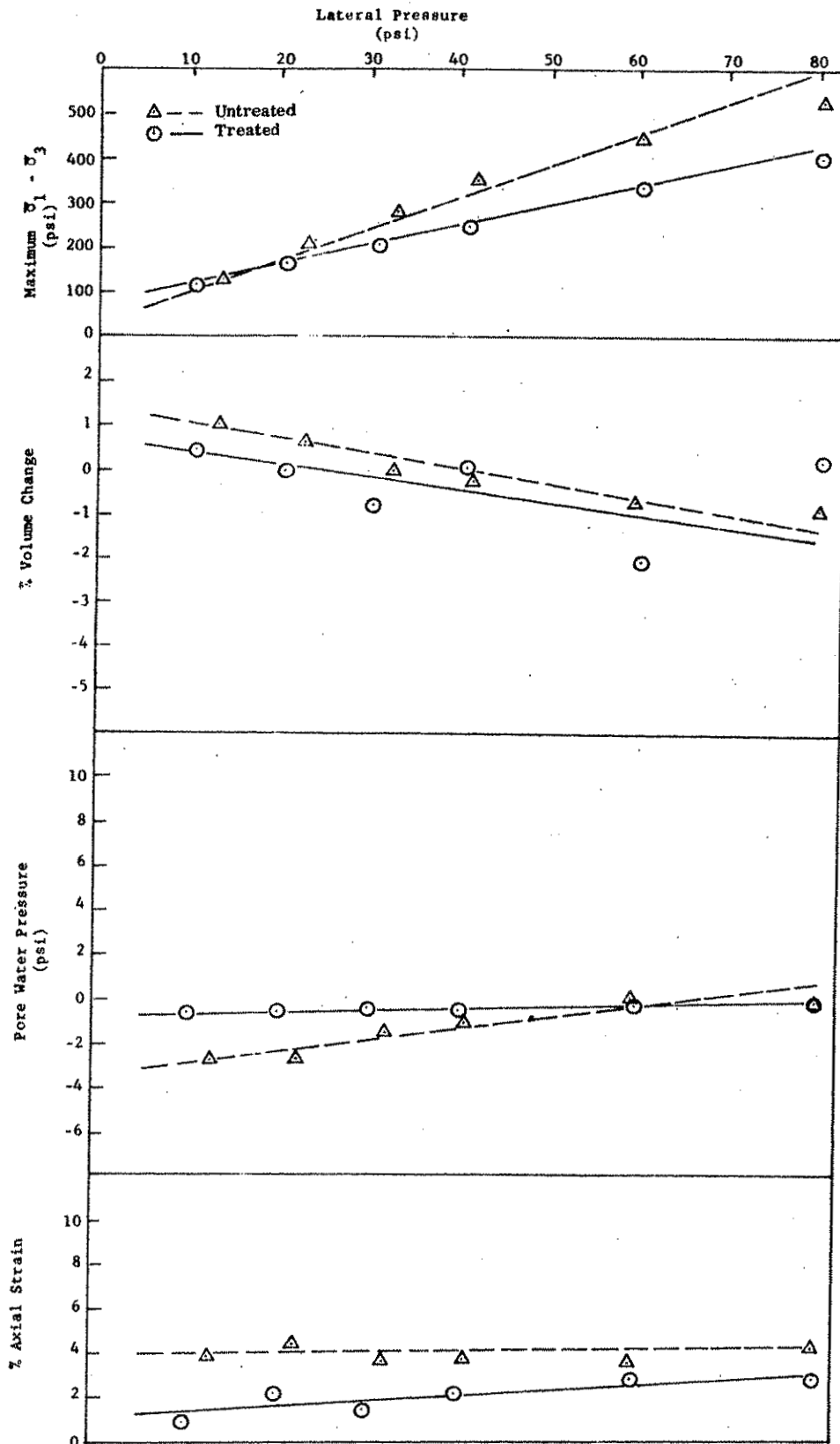
Figure 28.   Percent volume change, pore water pressure, and percent axial strain, at maximum deviator stress for untreated and asphalt cement treated Garner specimens tested at varying lateral pressures

high and low lateral pressures. By reducing high pore pressures, the treatment increased the shear strength of the stone, and, by reducing negative pore pressures, the treatment lowered potential suctions that would contribute to capillary moisture rise within a base course material. Gilmore and Garner stones, being less porous than the Bedford stone, exhibited slight improvement in pore pressures upon treatment with the two asphaltic additives.

4. Reduction of axial strain at maximum deviator stress may be one criterion of base course stability. At lower confining pressures, the bituminous treatments significantly lowered the percentage of axial strain needed to achieve maximum $\bar{\sigma}_1 - \bar{\sigma}_3$. Reduction of strain is probably effective in reducing deformation and rutting of base course mixes, as long as low lateral pressures are maintained and maximum deviator stresses are not exceeded. At higher lateral pressures the treated Bedford and Gilmore stones showed greater axial strain at maximum $\bar{\sigma}_1 - \bar{\sigma}_3$ than the untreated materials, indicating a lowering of stability.

As previously mentioned, minimum volume of the untreated and Portland cement treated stones occurred at a stress level less than the point of either maximum effective stress ratio or deviator stress. Minimum volume of the bituminous treated stones generally occurred after the achievement of maximum effective stress ratio. It is theorized that this minimum volume lag may have occurred due to one or a combination of the following factors:

a. Though failure may occur due to shear of the specimen along the weakest plane, not all of the soil grains within the specimen have achieved complete contact due to the asphaltic film separation. As the axial load is increased beyond maximum effective stress ratio,

.the additive will flow until the soil grains are in complete contact.
As the soil particles re-orient, the volume begins to increase.

b.   The observed minimum volume lag was greater for specimens treated
with a 4% (Asphalt cement treated) additive than for those treated with
a 3% (SS-1 emulsion) additive. Increased asphalt content plus some-
what higher test temperatures associated with the AC treated specimens
may increase the volume change lag.

c.   Throughout the project, a rate of axial deformation of 0.01 in.
per minute was used on all triaxial test specimens. To enable shear
to occur at particle to particle contact, rather than through any
asphalt film and prior to development of maximum effective stress
ratio, an axial deformation rate less than 0.01 in. per minute should
have been used.

The following are recommendations based on tests and analyses
performed:

1.   At low confining pressures there appears to be an increase
in stability for the bituminous treated stones. Treatment of the three
stones was the most effective with the poorer quality Bedford due to
reduction of capillary moisture rise within the base course mixture. With
the better quality and less porous Gilmore and Garner stones, asphalt
contents of 1 or 2% might be sufficient for achievement of waterproofing,
while stability of the mixtures would then be dependent on the mechanical
stabilization. Baskin and McLeod (1940) have discussed such a concept.

2.   In accordance with similar procedures used in this study, tests of
specimens treated with asphalt cement contents of 1 or 2% should be

conducted to determine variations in stability corresponding to the reduced

AC content.

3.   Further studies should be conducted to analyze the volume change

lag phenomenon, with a repetitive axial load triaxial shear test utilized

early in the investigation.   It is anticipated such a test may indicate a

decrease of volume change lag through cyclic axial loads.

C.   Treatment with Sodium Chloride, Calcium Chloride, and Hydrated Lime

Reference is made to the work of Wassenar, Handy and Hoover[9] for a

detailed analysis of this portion of the problem area.

Because of the mixed service record of the Bedford stone, it was selected

for treatment with calcium or sodium chloride in amounts of 0.5% by dry

weight of aggregate in accordance with NaCl content recommendations of the

Salt Institute.   All three stones received lime treatment levels of 1.0

and 3.0%, and further tests were conducted on the Bedford and Garner

stones with 10.0 and 16.0% lime.

To evaluate angle of internal friction φ' and cohesion c' the failure

point was defined as the maximum effective stress ratio, $(\bar{\sigma}_1 - \bar{\sigma}_3)/\bar{\sigma}_3$.   Methods

of analysis utilized were the Mohr envelope, Bureau of Reclamation, and stress

path methods previously described.   Maximum ordinate points for the stress

path method conformed very closely to straight lines for all series of tests

and was used in subsequent analyses.

Possible changes normally expected in physical properties of chloride

treated stones are: (1) increase in dry densities due to increase in surface

tension and lubrication as an aid to compaction; (2) increase in moisture

retention; (3) flocculation of clay particles, improving permeability; (4)

improvement in interlocking due to recrystallization of sodium chloride; and

(5) lowering the freezing point of the treated material.

Effective shear strength parameters, φ' and c', for the untreated

Bedford stone were 44.7$^{\text{o}}$ and 9.6 psi respectively. For the sodium-chloride-

treated stone the values were 43.6$^{\text{o}}$ and 11.2 psi, and for the calcium-chloride-

treated, 46.3$^{\text{o}}$ and 7.2 psi. The addition of NaCl therefore caused a very

slight decrease in φ' with a slight increase in c', whereas the opposite

effect was noted with the $CaCl_2$ treatment. These changes are considered to

be of negligible proportions.

Maximum pore water pressures occurred near failure in all untreated

samples. In general, maximum pore pressures were lower in the NaCl treated

specimens and tended to be lower in the specimens treated with $CaCl_2$. Since

φ' and c' were calculated on an effective stress basis this does not directly

influence the previous conclusions. However, if extrapolation to the much

higher rates of loading in actual highways is made, reduction in pore

Figure 29 presents stress moduli[*] versus lateral pressure for the Bedford

stone with and without chloride treatment. For comparison, data for untreated

Bedford at modified and standard compaction are also presented. Lines fitted

by method of least squares are shown and correlation coefficients are indicated.

Modified compaction obviously increases rigidity of the Bedford stone, being

much more effective for this purpose than the use of either chloride additive.

The stress modulus at standard compaction increases with lateral pressure,

---

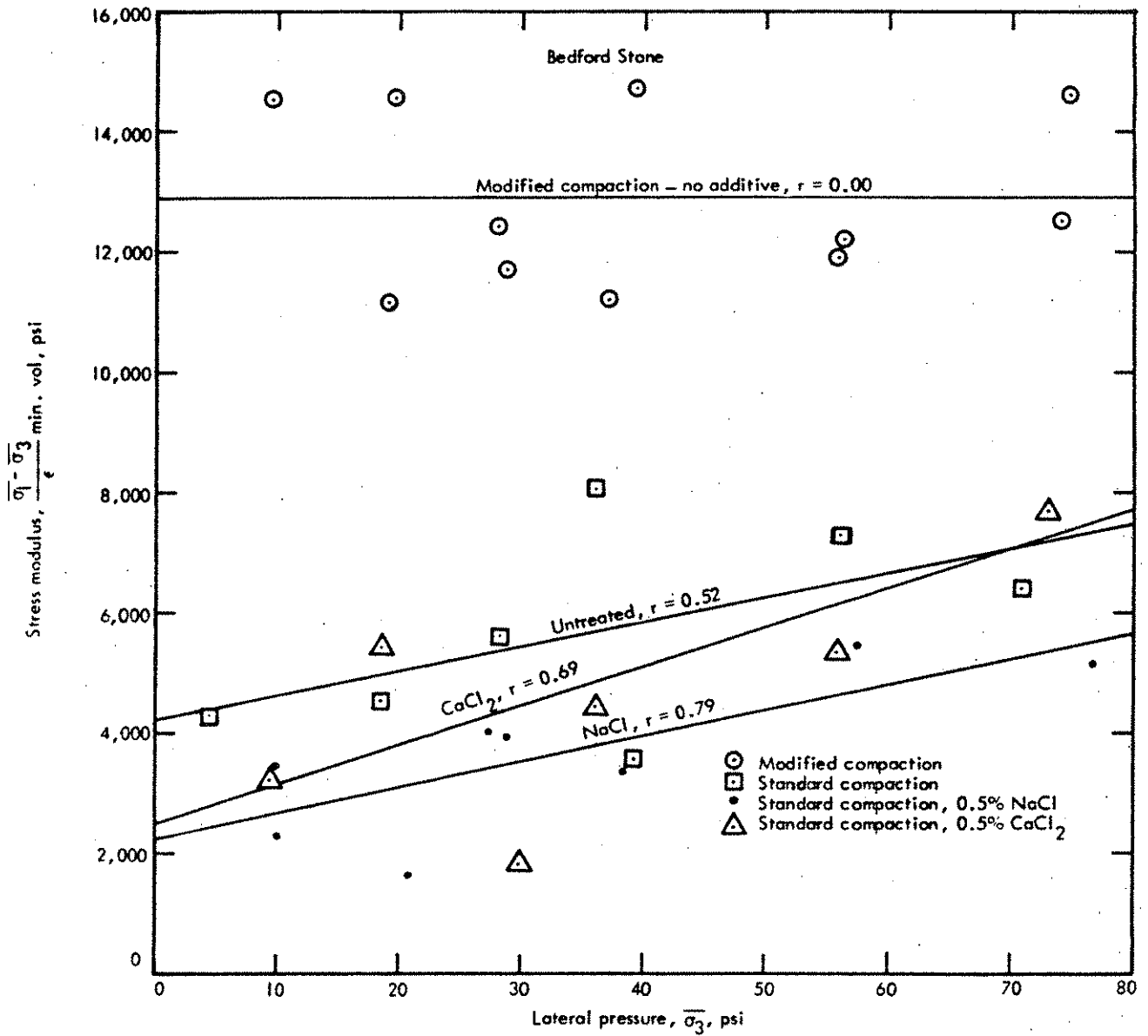[*]Stress moduli was defined in section B-4 of Problem 2.

Fig. 29. Stress modulus indicating rigidity of compacted Bedford stone
with and without chloride treatments. Correlation coefficients
(r) are for the relationship to lateral pressure.

indicating consolidation, whereas the specimens after modified compaction apparently resist further consolidation. Addition of chlorides caused minor decreases in the stress modulus from those values of the untreated and therefore were of no benefit.

Optimum lime contents for the three crushed stones were determined by unconfined compression tests performed on 2-in. diam by 2-in. high cylinders. Only that fraction of each material passing the No. 10 sieve was used in this test. Optimum moisture contents at each percent lime were determined for all three stones, and duplicate test specimens for each lime content were then molded by drop hammer compaction. Following 28 days moist curing the specimens were tested in unconfined compression at a rate of deformation of 0.1 in. per minute. A plot of **load versus calcitic lime** content was made to indicate optimum lime content for the minus No. 10 materials. The lime content was then corrected to a whole soil basis. Based on the above results, 1 and 3% lime were selected as trial percentages for triaxial testing with a few additional tests at 10 and 16% lime to insure a maximum pozzolanic reaction.

Based on plasticity and clay mineralogy of the stones, lime treatment was expected to be most effective with the Bedford. Action of hydrated lime is first to improve flocculation of clay into silt-size aggregate and should be reflected in an increase in φ' and decrease in c'. Second, lime and clay participate in a long term pozzolanic reaction that should increase c'. Lime produced the anticipated results on the Bedford stone by decreasing c' at 7 days and increasing it at 90 days, indicative of flocculation followed by cementation; i.e., with only 1% lime, c' went from 9.6 to 16.2 psi.

Simultaneously the reverse occurred in φ', but was less than 2°. With 3% lime, similar effects were more noticeable, and 10% lime produced a c' of 24.6 psi after only 28 days.

Lime decreased density of the Bedford, another indication of flocculation. At the 3% level, lime greatly increased pore pressures during testing, suggesting reduced permeability due to plugging of pores by unreacted lime. With longer curing the effect diminishes, presumably as the lime is used in pozzolanic reaction.

One percent lime decreased density of the Garner, reduced c' and also φ' suggesting that lime acts as an inert lubricant. Addition of lime still resulted in higher pore pressures, reinforcing the conclusion of pore plugging of unreacted lime.

Probably because of similar clay mineralogy (Tables 1 and 2) the Gilmore stone behaved in much the same manner as the Garner.

As shown in Fig. 30, addition of 1% lime to the Bedford stone had no influence on the stress modulus after 7 days cure. After 60 days curing, the modulus was appreciably higher, suggesting greater rigidity through pozzolanic reaction. At 3% lime, stress moduli were about the same as with the untreated Bedford, probably because the benefit from pozzolanic reaction was offset by higher pore pressures caused by the excess lime.

Following is a summation of the conclusions pertaining to the chloride and lime treatment study:

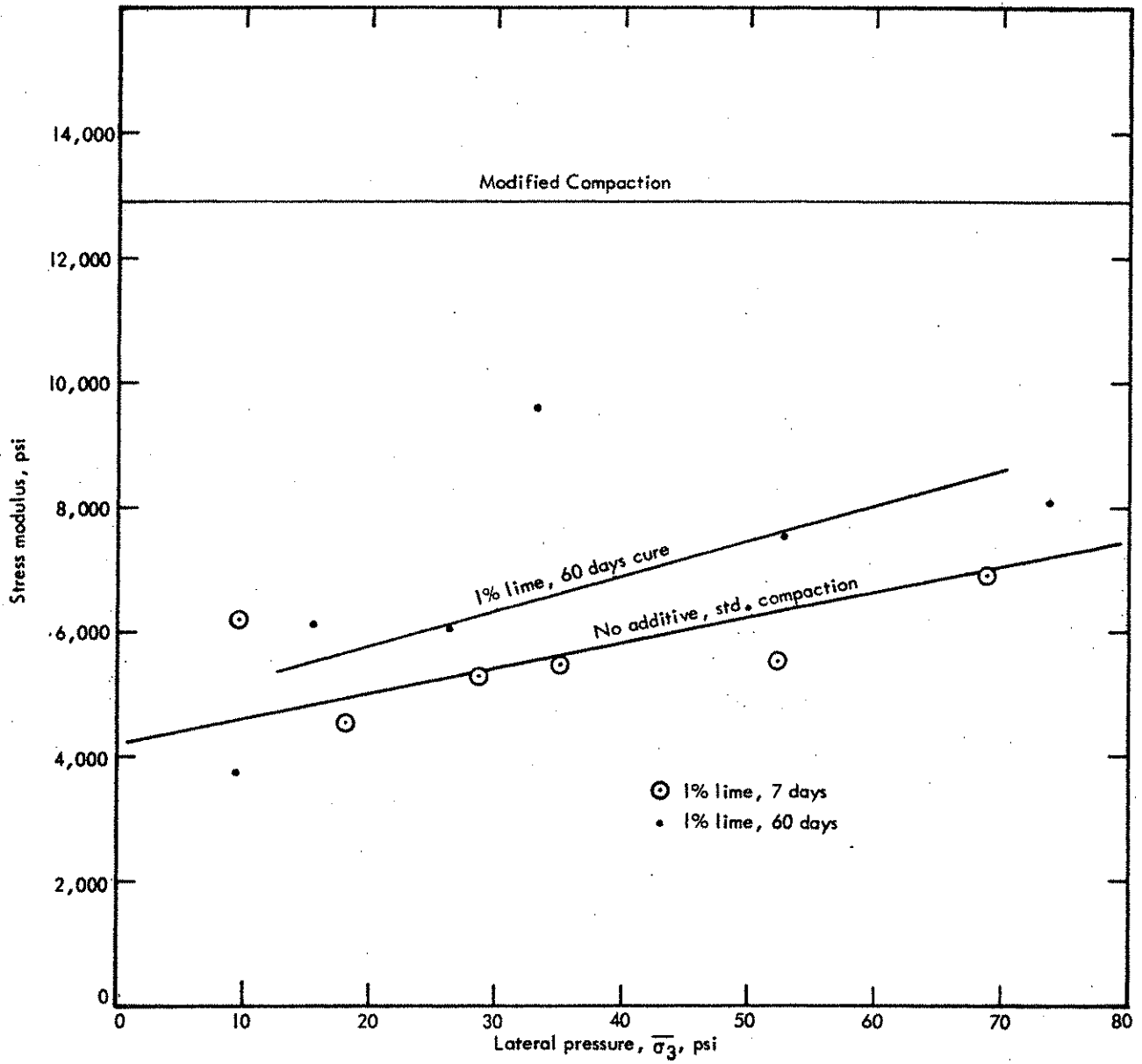1. An attempt to improve the Bedford stone with additions of 0.5% NaCl or $CaCl_2$ gave the following results:

Fig. 30. Stress moduli for selected lime-Bedford stone mixes.

a. NaCl decreased φ' slightly and increased c' about 17%.

b. CaCl$_2$ acted oppositely; it increased φ' slightly and decreased c' about 25%.

c. Both additives tended to decrease rigidity of the compacted stone.

Since the strength benefits are small, use of these additives in the proportions investigated is not recommended where the goal is an increase in strength.

2. Treatment of the stones with hydrated lime benefited only the Bedford stone, probably because of its higher content of clay, primarily kaolinite.

a. A curing time of 28 days or longer was necessary to gain a beneficial reaction.

b. Shorter curing times and/or excess unreacted lime caused significantly higher pore pressures, perhaps due to plugging of pores by lime.

c. The main benefit from lime was to increase cohesion. Addition of 1% lime increased c' as much as 70% after 90 days curing. The friction angle was not significantly affected, even though compacted density was somewhat reduced.

d. With low lime content and long curing, lime treatment increased rigidity. Otherwise there was no affect.

Use of lime to improve the strength characteristics of crushed stone does not appear justified at this time. Two potentially deleterious side effects are lower compacted density and higher pore water pressures.

D. Treatment with an Organic Cationic Waterproofer

The purpose of this portion of the problem area was to determine the ability of Arguard 2HT* to waterproof and potentially improve the immersed shearing resistance of the Bedford crushed stone.

Reference is made to the work of Demirel, Farrar and Hoover[10] for a detailed analysis of this portion of the problem area.

Since pavement loads are transient, it is doubtful whether drainage of the treated material would occur during an instantaneous load-unload cycle. Thus a quick (unconsolidated-undrained) triaxial shear test was used to measure cohesion c and angle of friction φ of the untreated and treated Bedford material. No volume change or pore pressure measurements were made.

Standard solutions of Arquad 2HT were prepared as a dispersion in distilled water heated to a temperature of 60°C. Thus prepared, they contained 7.5% of active Arquad on a weight basis. After cooling, the desired quantities of Arquad 2HT, as a percentage of the total weight of the mix, were added to the crushed stone. Additional distilled water was added to provide the desired moisture content.

There was a general decrease of density and optimum moisture content with increasing amounts of Arquad 2HT as summarized below:

---

*Commercial trade name of a dioctadecyl dimethyl ammonium chloride produced by Armour Industrial Chemical Company, Chicago, Ill.

Arquad 2HT content (% oven dry soil wt)	Maximum dry density (pcf)	Optimum moisture content (% oven dry soil wt)
0.00	130.5	10.7
0.02	128.5	10.7
0.05	128.5	10.6
0.10	127.5	10.1

One possibility for the decrease in density and OMC is that Arquad 2HT causes aggregation of the smaller particles, creating slightly poorer gradation and resulting in lower density.

To determine the moisture content range to which the treated stone should be air-dried to obtain the highest immersed shear strength, each specimen was molded at standard density in a CBR mold and air-dry cured for varying periods of time. All molded specimens contained 0.05% Arquad 2HT. Following determination of the air-dry moisture content, each specimen was tested by soaked CBR. Length of air-drying based on maximum practical moisture content loss during curing and highest soaked CBR value was selected as the curing period for treated samples in the major phase of the study. The following table summarizes the results:

Moisture loss during curing (% dry soil wt)	Soaked CBR at 0.1 in. penetration	Soaked CBR at 0.2 in. penetration	Saturation (%)	Vol. change during immersion[a] (%)
0.00	29.7	38.2	85.1	− 0.02
1.22	42.0	45.3	81.7	− 0.04
2.40	26.7	33.0	91.4	− 0.36
3.84	37.2	47.3	90.6	− 0.28
5.30	48.2	55.7	90.7	− 0.14
5.75	41.0	44.5	92.3	+ 0.88
6.27	31.5	36.7	83.9	− 0.12

[a]Based on the change in height as a percent of the original height, (−) indicates shrinkage and (+) indicates expansion.

Maximum immersed CBR indicated a necessary period of drying to produce a moisture content loss of about 4.5 to 5.8% by dry soil weight. Maximum saturation during immersion ranged from 81.7 to 92.3%, increasing to the maximum (at a moisture loss during curing of less than 6%), then rapidly decreasing due to additional air-drying substantiating the maximum practical air drying period. Volume change varied from a contraction of 0.36% to an expansion of 0.88%, showing little volume change due to immersion. All triaxial test specimens were thus air-dried to the above moisture loss range.

Four-inch diam by 8-in. high cylinders were molded with amounts of Arquad 2HT varying from 0.00 to 0.05%, air-dry cured until moisture loss was within the range previously noted, soaked with water for 48 hrs, and quick triaxially shear tested.

In order to retain the cylindrical dimensions of the specimens during

saturation, each specimen was molded inside a triaxial membrane by the vibratory method. Due to the addition of the rubber membrane in the mold, the method produced specimens at 92% of the maximum dry density obtained in the standard Proctor density tests. Higher densities were obtainable by using longer periods of vibration (5-10 minutes) but created definite segregation of coarse and fine materials in each specimen.

Following air-dry curing in the membranes, each specimen was placed in a water tank with water level maintained at 1/2 in. above the specimen top. A porous stone at the base of the specimen allowed water to infiltrate while a metal band inside the top of the membrane prevented its collapse and allowed the upper face of the specimen to be exposed to air. Following saturation each specimen was allowed to drain for 10 minutes before placement in the triaxial shear apparatus.

As noted in the table below, φ is considerably less for the untreated and treated material than reported in preceding sections of this report. This is due to (1) density achieved by the compaction procedure and (2) type of triaxial shear test, which did not account for volume change, pore pressure or other potential variables of analysis.

Mohr-Coulomb shear diagrams of the treated material showed circles and envelopes of failure that were fairly consistent and yielded about the same results for the different percentages of treatment. By comparison, results of the untreated material were very erratic, i.e., a linear envelope of failure could not be drawn. As a result, average values of apparent angle of friction and cohesion of the untreated specimens were obtained by applying the Bureau of Reclamation porcedure previously noted.

Arquad 2HT content (% dry soil wt)	Apparent angle of internal friction (φ) (degrees)	Apparent cohesion (c) (psi)
0.00	16.5	11.7
0.01	23.1	4.5
0.03	22.7	7.5
0.05	24.3	5.9

While φ for the treated specimens showed a definite increase from that of the untreated, the reverse occurred for cohesion. This characteristic further reflects an aggregation of the smaller particles due to the chemical treatment. Comparison of the average treated values of φ and c, at 23.4° and 6 psi, with the untreated probably represents only a general maintenance of the overall stability of the Bedford material.

During soaking it was noted that all treated specimens had free water on their tops within one hour. Similar saturation was noted for some of the untreated specimens, but for the remainder water did not rise to the specimen top. Three untreated specimens were then tested at lateral pressure of 60 psi and showed maximum axial stresses of 120, 140 and 156 psi. Water had appeared on the top of the first two specimens, but not on the third. In other cases where untreated specimens were tested at duplicate lateral pressures, the specimens not showing free water at the top also gave higher maximum axial stresses.

Quantity of moisture absorbed during soaking showed minimal variation between treated and untreated specimens and was measured primarily by variation in weight of the specimens after curing as compared to

weight following soaking and draining. Average weight of moisture absorbed by the untreated specimens and their standard deviation was 206 $\pm$ 49 g. Treated specimens absorbed 261 $\pm$ 27 g for 0.01%, 266 $\pm$ 7 g for 0.03% and 264 $\pm$ 13 g for 0.05% treatment.

The above situation indicates the extreme variation in water absorption and in possible pore water pressure of the untreated specimens, whereas the absorption and thus the potential pore pressures of the treated specimens were more uniform. It appears that Arquad 2HT treatment of the Bedford material limits the amount of absorbed moisture to the large pores. The rapid movement of water during the soaking phase indicates a general increase in permeability by treatment with Arquad 2HT.

In summary, use of Arquad 2HT to improve the overall stability of the Bedford stone does not appear amply justifiable at this time.

VI. ACKNOWLEDGMENTS

Darwin Fox, Al Whigham, Brad Moses, Milo Eckles, Jerry Spicer, Tom Leuschen,

Chuck Powell, and Mike Lindebak, all civil engineering undergraduate

students, who have assisted as laboratory technicians at various periods

throughout the project.

VII. SELECTED BIBLIOGRAPHY

1. Tinoco, F. H. and Handy, R. L., "Shear Strength of Granular Materials," Special Report, Engineering Research Institute, Iowa State University, Contribution No. 67-9 of the Soil Research Laboratory, 1967.

2. Bowden, R. P. and Tabor, D., The Friction and Lubrication of Solids, Oxford University Press, London, 1950.

3. Horn, H. M., "An Investigation of the Frictional Characteristics of Minerals," Ph. D. thesis, Department of Civil Engineering, University of Illinois, Urbana, 1961.

4. Taylor, D. W., Fundamentals of Soil Mechanics, Wiley, New York, 1948.

5. Best, T. W. and Hoover, J. M., "Stability of Granular Base Course Mixes Compacted to Modified Density," Special Report, Engineering Research Institute, Iowa State University, Contribution No. 66-15 of the Soil Research Laboratory, 1967.

6. Merrill, D. C. and Hoover, J. M., "Laboratory Freeze-Thaw Tests of Portland Cement Treated Granular Bases," Special Report, Engineering Research Institute, Iowa State University, Contribution No. 67-2 of the Soil Research Laboratory, 1967.

7. Ferguson, E. G. and Hoover, J. M., "Improvement of Granular Base Course Materials with Portland Cement," Special Report, Engineering Research Institute, Iowa State University, Contribution No. 67-3 of the Soil Research Laboratory, 1967.

8. Whisler, J. C. and Hoover, J. M., "Stability of Granular Base Course Materials Containing Bituminous Admixtures," Special Report, Engineering Research Institute, Iowa State University, Contribution No. 66-16 of the Soil Research Laboratory, 1967.

9. Wassenaar, A. G., Handy, R. L., and Hoover, J. M., "Lime or Chloride Treatment of Granular Base Course Materials," Special Report, Engineering Research Institute, Iowa State University, Contribution No. 67-8 of the Soil Research Laboratory, 1967.

10. Demirel, T., Farrar, M. H., and Hoover, J. M., "Treatment of a Crushed Stone with Quaternary Ammonium Chloride," Special Report, Engineering Research Institute, Iowa State University, Contribution No. 64-10 of the Soil Research Laboratory, 1965.